Collapse analysis of the Clock and Fortified towers of Finale Emilia, Italy, after the 2012 Emilia Romagna seismic sequence: Lesson learned and reconstruction hypotheses

Maurizio Acito [a,b], Claudio Chesi [a,b], Gabriele Milani [a,b,*], Stefano Torri [a,b]

[a] *Department of Architecture, Built Environment and Construction Engineering ABC, Italy*
[b] *Technical University of Milan, Piazza Leonardo da Vinci 32, 20133 Milan, Italy*

In the present paper, different full 3D FE numerical models exhibiting increasing levels of complexity are presented, to have both an insight into the causes of collapse of the Finale Emilia Clock and Fortified Towers in occasion of the 2012 Emilia Romagna, Italy, seismic sequence and propose effective reconstruction strategies. Two hypothetical rehabilitation interventions implemented before the earthquake sequence (which could be utilized as reference for a future reconstruction), one made with lime mortar restoration and the other with cement mortar deep repointing with injection, are evaluated from a seismic point of view. The numerical assessment includes modal analyses, a simplified procedure provided by the Italian Code for the Built Heritage, non-linear static (pushover) and full non-linear dynamic analyses. In all cases, full 3D realistic FE models derived from detailed geometric virtual models of both towers are used. Within the non-linear static and dynamic analyses, a damage plasticity model with distinct damage parameters in tension and compression is adopted. From the numerical results, both the role played by the actual geometry and the insufficient resistance of the original masonry material are addressed, also in light of the actual failure mechanisms observed. By quantitatively comparing the efficiency of the two methodologies of rehabilitation considered, it is found that very little damage develops when lime mortar is used, whereas less effective results are obtained when injections with cement mortar are used.

Keywords:
Masonry towers
Pushover
Non-linear dynamic analyses
May 2012 Emilia Romagna earthquake
Rehabilitation and reconstruction

1. Introduction

On the base of what happened on May 20–29th 2012 in Emilia-Romagna (Italy), following the strong earthquake that struck that region, many studies have been conducted to investigate the damage of some monuments belonging to the Italian cultural heritage and to extract useful information about the possibility of future reconstruction of damaged buildings.

This research is conducted by the authors in cooperation with the Italian Cultural and Architectural Heritage Ministry (MiBAC) with the support of Finale Emilia municipality.

In this paper the Clock Tower (Fig. 1(a)) and the Fortified Tower of the Rocche Castle (Fig. 1(b)) are analyzed with sophisticated numerical models.

Both structures are located in Finale Emilia (Italy) [1], within the seismic crater, and both suffered serious damage that compromised

* Corresponding author.
E-mail address: gabriele.milani@polimi.it (G. Milani).

©2016. This manuscript version is made available under the CC-BY-NC-ND 4.0 license http://creativecommons.org/licenses/by-nc-nd/4.0/
Published Journal Article available at: http://dx.doi.org/10.1016/j.conbuildmat.2016.03.220

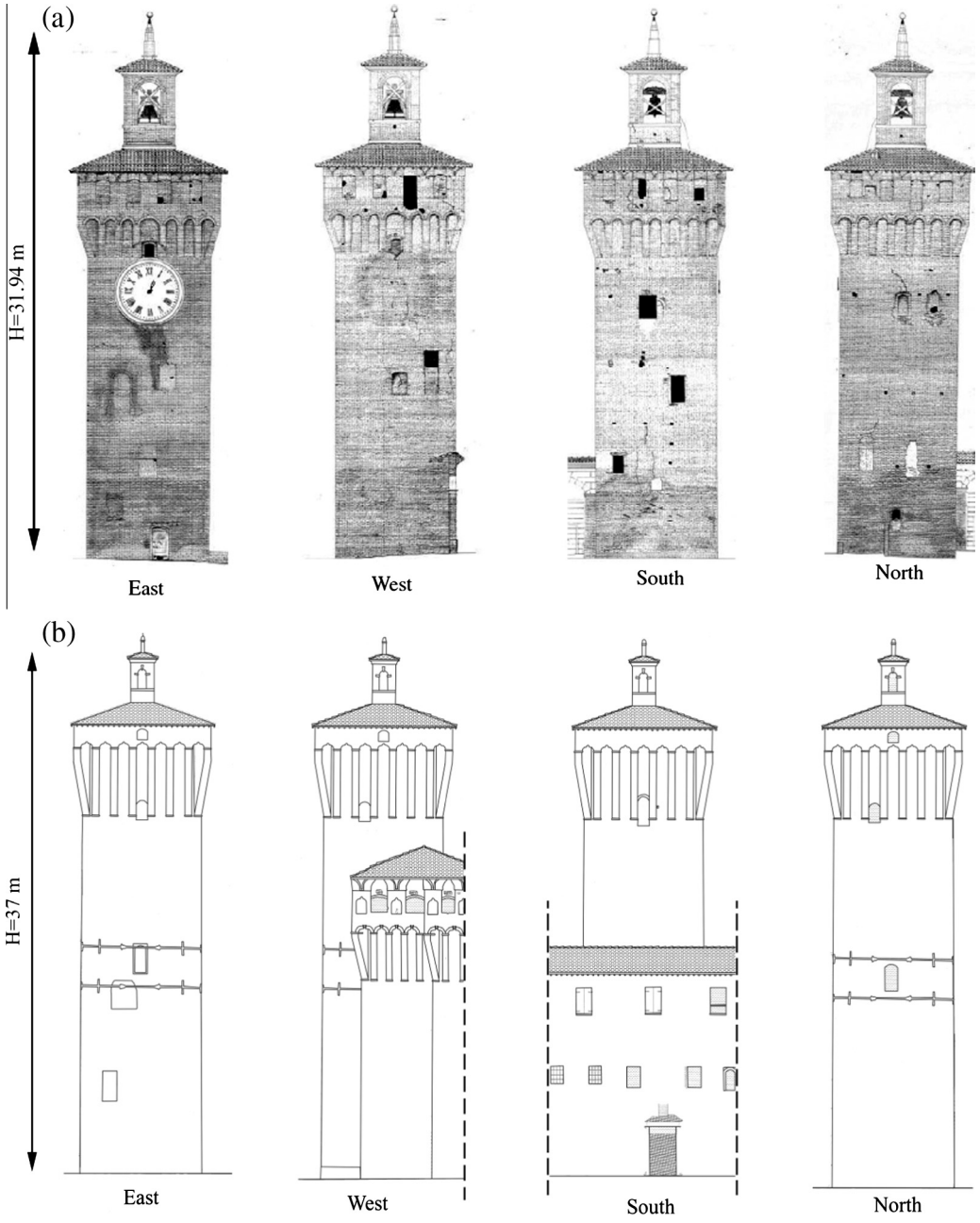

Fig. 1. Lateral schematic views of the Clock Tower (a) and the Fortified Tower (b).

their stability at a point that they collapsed few hours after the seismic event occurred on May 20th.

After the main shock, the clock-tower was split into two parts: one collapsing immediately, the other standing precariously and collapsing during the subsequent strong aftershock. The Fortified Tower of the castle suffered total collapse at an early stage of the first shake.

Different numerical models have been analyzed in detail to investigate the seismic behavior of both the towers by means of different numerical strategies (including non-linear static and dynamic analyses) as well as the reasons that caused the collapse.

Subsequently, the same numerical analyses are performed under two different hypothetical situations of material restoration. In this way, it is possible to ascertain if the collapse could have been avoided with suitable interventions and which restoration strategy is the most effective for such a kind of structures.

The investigation deals with the hypothetical analysis of the towers after a suitable rehabilitation intervention done before the seismic sequence, that was not implemented in reality but that could have drastically changed the performance of both the towers against horizontal loads, partially preserving their integrity and precluding total collapse.

In particular, two different consolidation methods are considered in the analysis and the consequent seismic performance critically evaluated.

The first consists in the restoration of the original stiffness and strength properties of the masonry walls (constituted by lime mortar and clay bricks) by substituting the degraded material with mortar presenting the same characteristics as the historical one, improving transversal connection between the different wall leafs and corner interlocking.

The second consolidation method takes into account the combined effect of injections with deep repointing using cement

mortar, a material exhibiting however different mechanical characteristics from the original one.

The mechanical properties adopted in each analyzed case are tuned with reference to appropriate experimental works conducted by different authors on similar quality masonry.

The analyses performed to investigate the three different situations include the evaluation of the vulnerability indices according to the Italian Guidelines for the architectural heritage by means of response spectrum and linear static analyses. The latter is performed with respect to both the design spectrum prescribed by the Italian Code and that corresponding to the time history associated to the 2012 seismic event.

Non-linear three dimensional pushover analyses along the two inertia directions have been also carried out, in order to compare the seismic demand in terms of inelastic acceleration–displace ment with the 1 DOF equivalent response. A sophisticated damage-plasticity model available in the commercial FE code ABAQUS is utilized in order to account for some of the distinctive features of masonry, as the limited tensile strength, the softening behavior and damage properties both in tension and compression.

When dealing with the pushover results, comprehensive sensitivity analyses varying the mechanical parameters of the non linear constitutive model are presented.

Finally dynamic analyses based on the original ground motion recorded for the May 20th event in Mirandola have been conducted with the same damage-plasticity model adopted for the pushover analyses. Both horizontal and vertical components of motion have been applied. The analyses take into consideration both geometrical (large displacement effects) and material (elasto plastic damage behavior in both tension and compression for masonry) non-linearity.

2. Main features of the May 2012 seismic event

As it is well known, the seismic sequence of May 2012 caused severe damage to many historical masonry buildings and monuments (churches, bell towers, palaces), in the provinces of Modena, Ferrara and Mantua.

On May 20th, 2012, at 02:03:53 (UTC), the aforementioned area was stricken by an earthquake of magnitude $M_L = 5.9$ (lat 44.890 long 11.230, ipocentral depth 6.3 km).

The main shock was preceded by a $M_L = 4.1$ event on May 19th and followed by four relevant aftershocks with $4.8 < M_L < 5.1$ in the following days: two events with $M_L = 5.1$, one with $M_L = 4.9$ and one with $M_L = 4.8$. Eleven events with magnitude $4.0 < M_L < 4.5$, plus several other minor earthquakes, occurred in the same area between May 20th and May 23th, as reported by the Italian

Fig. 2. Collapse sequence for the Clock Tower (a) and the Fortified Tower (b).

Instrumental and Parametric Data-Base (ISIDe) [http://iside.rm.ingv.it/iside/standard/index.jsp].

One of the earthquake most impressive effects is given by the collapse, following the main shock, of the Clock Tower and Forti-fied Tower in Finale Emilia, which are analyzed in this paper, see Fig. 2(a) and (b). The main shock of the sequence in May 2012, like many others with a magnitude between 4 and 5, were originated by earthquakes with epicenters few kilometers far from the Finale Emilia city center (the main of May 20th no more than 10 km to the North-West). The distribution of seismic events with a magni-tude greater than 5, along a broad front in the east-west direction, and extension of about 50–60 km, caused the collapse of many other historical buildings and churches in many small towns. Finale Emilia, for instance, suffered for serious damages of all the churches, bell towers, and for almost all the aggregates of the old part.

The current seismic zonation map by INGV [Interactive Seismic Hazard Maps, (esse1-gis.mi.ingv.it)], adopted by the current seismic design codes [2,3], specifies for the epicentral area, with a 10% exceedance probability in 50 years, an expected maximum horizontal acceleration approximately of 0.15 g on stiff soil, and of 0.22 g on C category soil (180 m/s < $V_{S,30}$ < 360 m/s). Globally, based on historical data, the seismicity of the area can be defined as medium-low. It is remarked that INGV has proceeded to the seismic re-classification of the Padana Plain in 2003 only [4], after the disastrous events of the San Giuliano earthquake in Puglia. Previously, this area was filed as non-seismic, and the first classification of the geographic zone interested by the earthquake events of May 2012 became effective since 2005 [5].

In Fig. 3, code of practice acceleration spectra for return periods Tr = 475 and Tr = 949 years are compared to the one relative to the MRN station [first mainshock, Mirandola station] [6]. Apparently, the occurred earthquakes are comparable to events corresponding to high return periods.

3. Material properties of masonry

As already pointed out, three cases are analyzed assuming different hypotheses on the mechanical properties of the masonry material.

The analyzed cases include the original historical masonry characterizing traditional buildings in Finale Emilia, and in particular the towers under consideration. This kind of material is associated to poor mechanical properties as it has been found during the inspections done after the seismic sequence by the authors [7]. Unfortunately, it was not possible to perform any experimental mechanical characterization on the tower rubbles, so mechanical properties of similar historical masonries, in agreement with Italian Code indications, are adopted in the models.

According to the Code, chapter 8, the mechanical properties to be assumed depend on the knowledge level (LC). Three different LCs are provided by the code, labeled from 1 to 3, related to the knowledge level available for the mechanical and geometrical properties of the structure. LC3 is the maximum, whereas LC1 is the minimum. For the case at hand, in the absence of specific in situ test results, the LC1 level is assumed.

In other reference cases, two hypothetical situations of different consolidation interventions on the masonry walls have been considered. The comparative analysis between such restoration hypotheses is of interest, as it provides an insight into the suitable way to proceed in reconstruction interventions, to oppose the kind of damage occurred during the 2012 seismic event and to preserve, in the future, the stability of the two structures from possible shakes with similar magnitude.

In particular, two different restoration interventions are critically compared. In the first one, the reconstruction with a masonry material exhibiting mechanical properties similar to the original ones (lime mortar and clay bricks) is considered, with the assumption of good transversal interconnection among leafs and at

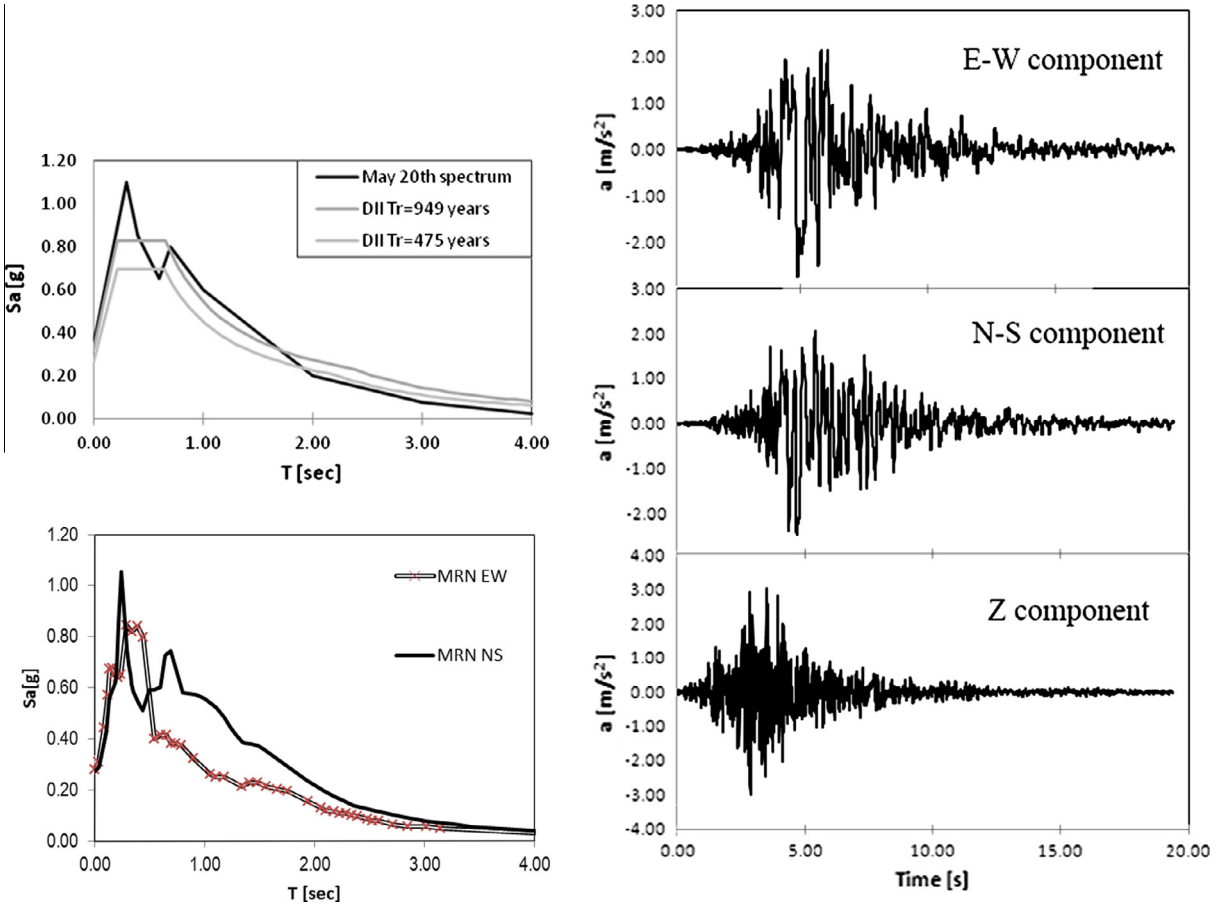

Fig. 3. Elastic code of practice spectra compared with that associated to the 20th May seismic event and real accelerograms used in the non-linear dynamic simulations.

the corner of interconnecting perpendicular walls. In this way, the conservation of the architectural features characterizing these historical structures is assured.

The second intervention makes use of combined techniques of injection and deep repointing by using cement mortar (a material with different mechanical properties with respect to the original ones) [8,9]. The invasiveness of this second approach is much higher, also because compatibility between pre-existing ruins and newly reconstructed parts is not safeguarded.

When dealing with non-linear static analyses, for each case considered, two non linear constitutive laws are assumed for the masonry material:

- An isotropic elastic-perfectly plastic material obeying a Mohr-Coulomb (MC) failure criterion [10] with associated flow rule, available in the commercial code Strand7 [11]. This is a particularly simple approach that can be used also at a professional level to deal with the pushover analysis of historical constructions. Apart elastic properties, it is necessary to define only two inelastic parameters, namely cohesion and the friction angle. Despite such a kind of approach does not allow for the reproduction of possible softening in the global pushover curve, it is however allowed by the Italian guidelines on the built heritage, because experts in this field are aware that (1) it is very difficult to obtain softening in the case of quasi-no-tension materials with complex 3D models where the self-weight plays a crucial role instead of the fracture energy in tension and (2) sophisticated software with robust arc-length routines is needed to deal with 3D elements and material softening.
- The so-called concrete damaged plasticity model (CDP) available in the commercial code ABAQUS [12]. This is a model with an isotropic constitutive law defined by different strength in tension and compression, elasto-plastic behavior with damage and softening ruled in tension and compression by two independent parameters, a 3D behavior obeying a Drucker-Prager failure criterion with vertex regularization and non-associated flow rule. The definition of the entire mono-axial $\sigma - \varepsilon$ relationship is needed [13]. Exhibiting the model damage in both tension and compression, it can be also used to perform non-linear dynamic analyses (see Fig. 4).

The matter of the practical definition of both constitutive laws is connected to the absence of experience on defining the tension limit strength of masonry [14]. This question is linked to the difficulties in performing accurate experi-mental tests to reproduce reliable values for tension strength in masonry specimens.

For this reason, an experimental campaign has been conducted at the Technical University of Milan [15,16] for the numerical characterization of the shear behavior in terms of Mohr-Coulomb parameters for lime mortar and clay brick masonry similar to the one that will be likely used during reconstruction.

Then, a calibration procedure of the parameters can be obtained through experimental data fitting, to be used in the concrete damage plasticity model at a structural level. The experimentation presented in [16] relies on direct shear tests conducted on bricks triplets, with different level of pre-compression applied at the top. The reader interested in further details on the experimental campaign is referred to [15,16].

The goal is obviously to provide an estimation of the Mohr-Coulomb failure surface and hence, masonry friction angle and cohesion.

The numerical procedure consists simply in defining realistic parameters for the models, to fit as close as possible the experimental output, by means of a trial and error method.

This procedure is repeated for all the types of materials considered.
When dealing with the concrete damage plasticity model, a simple three linear curve in tension is adopted, whereas the curve proposed by Kaushik et al. [17] is used to define the compression constitutive law. The reader interested in further details is referred to [18].

Such calibration is paramount in view of the non linear dynamic analyses conducted on the two towers. As a matter of fact, the dissipative and softening behavior in shear is needed for a proper prediction of the stiffness degradation, of the initial and residual strength, as well as to roughly estimate the dissipation properties associated to the cyclic hysteretic behavior.

3.1. Calibration of the mechanical parameters on historical masonry

No experimentation of samples extracted from in-situ rubbles is available in this case. In order to estimate the mechanical parameters for historic masonry, it is therefore convenient to refer to what stated in the Italian Code (Table C8A.2.1) for a low level of knowledge (LC1). For clay masonry with lime mortar the following parameters should be adopted: 2.4 MPa for masonry compressive strength and 1500 MPa for Young modulus.

3.1.1. Restored masonry

This consolidation procedure consists, in general, in the identification of the degraded elements and the subsequent replacement with similar materials. In this way, not only the original appearance of the structures is guaranteed but also initial mechanical properties are reconstituted.

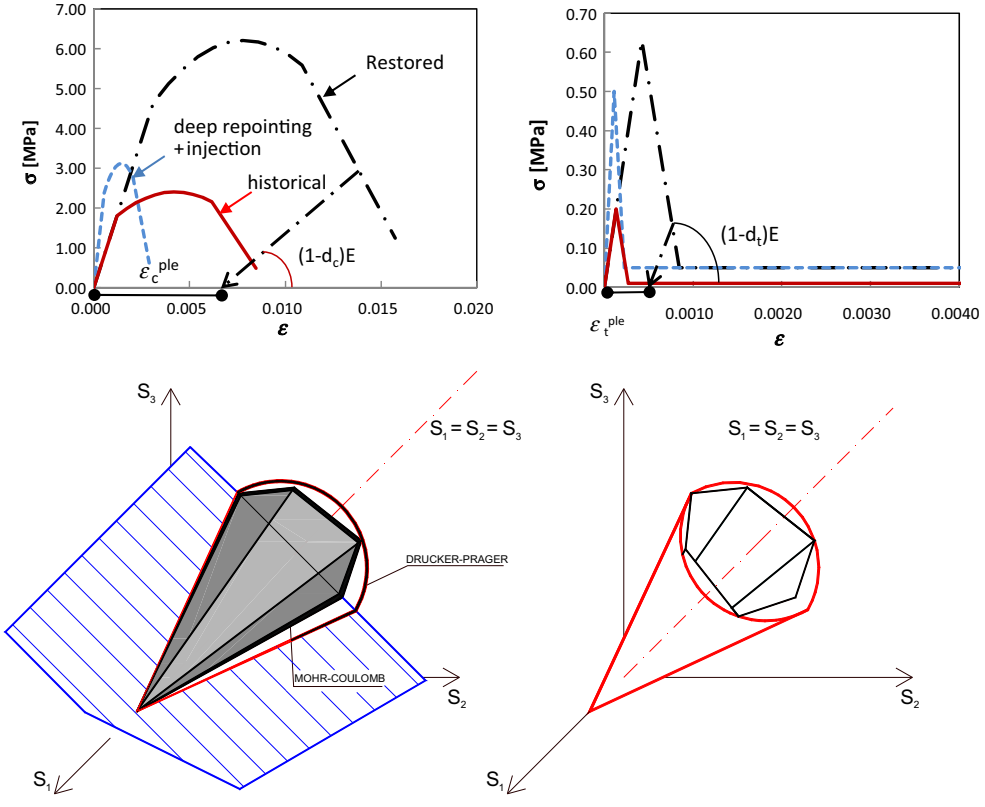

Fig. 4. ABAQUS CDP model non-linear behavior in uniaxial tension and compression (top) and regularization of the Drucker-Prager failure criterion in the Westergaard space (bottom).

To characterize the coefficients to be used within both MC and CDP models, reference is made to some existing direct shear tests conducted on historic masonry triplets in [15].

A preliminary characterization of the masonry material in compression revealed an average compressive strength value of 6.20 MPa (first cracks observed at 4.63 MPa) and a Young modulus value of 1491 MPa.

The shear tests are conducted on specimens constituted by three common historic Italian bricks (dimensions approximately 25 × 6 × 12 cm) joined by two layers of lime mortar 1 cm thick, see Figs. 5 and 6. Displacement is imposed on the lateral face of the central brick, under different vertical stress states, and is increased up to the formation of a failure mechanism. An indirect evaluation of the shear stresses on mortar joints is obtained experimentally by means of a load cell located at the same point where the horizontal displacement is imposed. From the envelope of all the shear stress-displacement relations so obtained, the parameters characterizing the Mohr-Coulomb failure criterion used within Strand7 have been estimated to be 0.33 MPa and 33.6° for cohesion and the friction angle, respectively.

By using the same calibration procedure for DCP plasticity, the values obtained for the mechanical parameters are 6.20 MPa and 0.63 MPa for the compression and tension strength, respectively.

The corresponding shear stress-displacement curves, numerically evaluated with the CDP model (on a homogeneous material representing macroscopically masonry as in Fig. 5-a, without vertical pre-compression and subjected to pure shear), are shown in Fig. 5c–d in case of historical and restored masonry.

Numerical analyses are made to check the real correspondence of the numerical output with experimental evidence. The real heterogeneous geometry of the experimental test is built into ABAQUS, imposing the same boundary and load conditions characterizing the experimental set up. Such a 3D model is constituted by 8631 nodes and 5600 brick elements, Fig. 6, with a mesh refinement at the mortar joints (double layer of elements along the thickness of the joints).

The prism is clamped at the base, an increasing displacement on the central brick lateral surface is applied at small increments up to the formation of a failure mechanism in the softening branch, far from the peak load. Different values for the vertical stress are assigned at the top face of the prism in order to simulate the different experimental setups, preventing in any case the rotation of the block by means of an extra layer of high stiffness elements, not shown in the figure for the sake of clearness.

A linear elastic material is used for bricks, while MC and CDP models are applied for joints. The goal is not only to compare the numerical results with experimental tests but also to show the difference between the two constitutive models. In particular, it is not expected to find a decreasing behavior of the post-peak curve for the elastic- perfectly plastic model.

Force-displacement numerical curves obtained with MC and CDP at the two levels of vertical compression experimentally investigated are compared to experimental evidence in Fig. 7. It can be seen that, for a realistic vertical stress state for a masonry tower (0.2 MPa), the difference between the numerical and experimental tests is fully acceptable from an engineering standpoint, even for the MC model, where softening is not present, however. Also the initial lateral stiffness is well approximated by CDP, whereas a stiffer behavior is observed for MC.

The presence of a reduced decreasing branch for MC simulations at 0.60 MPa of vertical compression is due to a geometrical non-linear effect, which may become relevant at high levels of pre-compression.

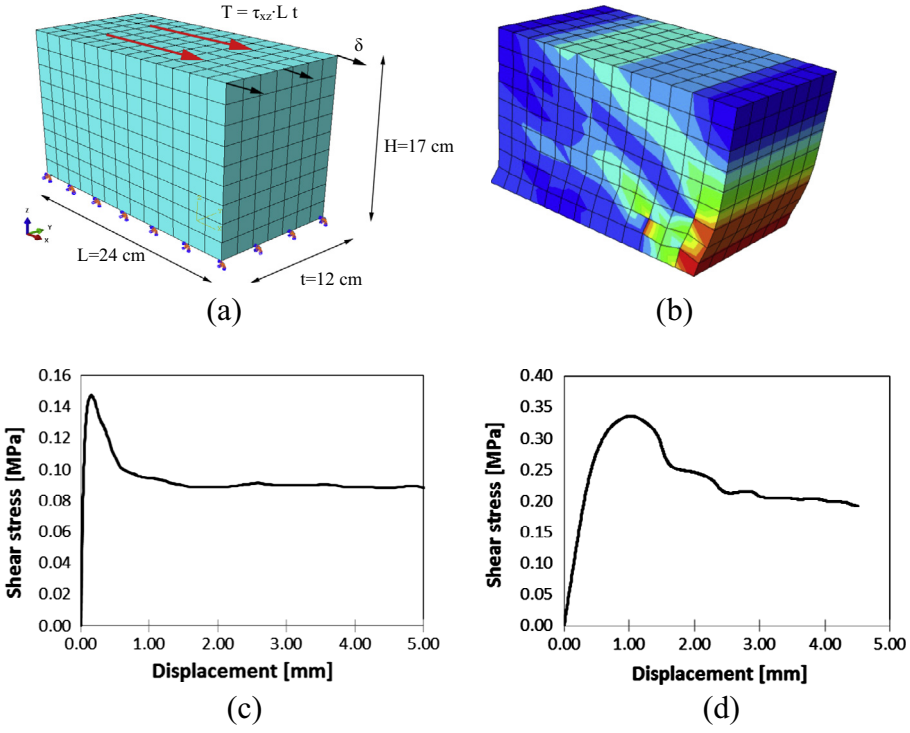

Fig. 5. Homogenous material (masonry) subjected to pure shear. Mesh (a), Von Mises stress distribution of the numerical sample used to calibrate the CDP material model (b) and the shear stress-displacement numerical curves obtained with calibration of the CDP model for historical masonry (c) and the restored one (d).

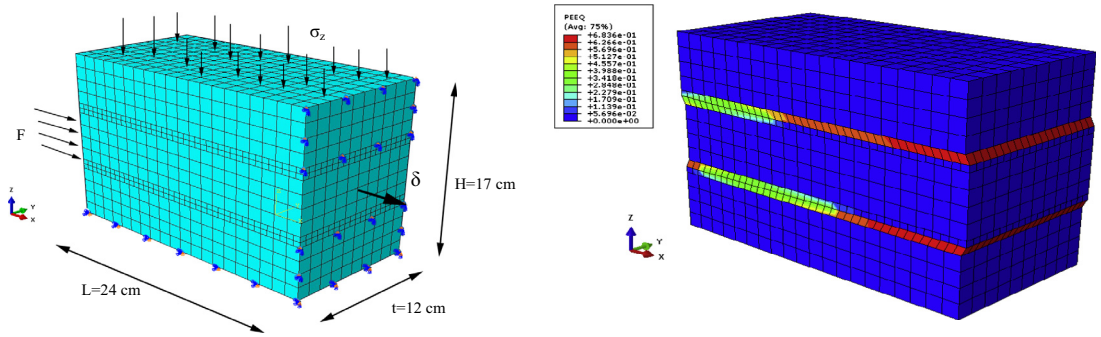

Fig. 6. Mesh and plastic strain distribution on the shear triplet.

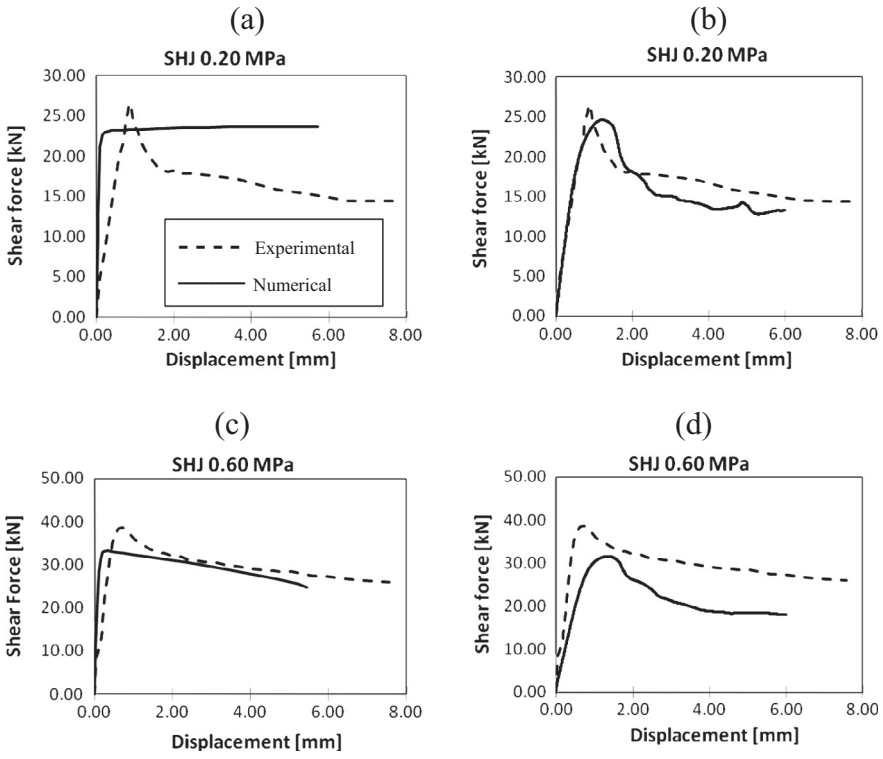

Fig. 7. Comparison between experimental and numerical analysis results: (a)-(c) MC failure criterion, (b)-(d) CDP constitutive law.

Increasing the vertical stress state, the fitting quality of the numerical output slightly decreases. Such discrepancy is most likely due to the development of plastic deformation in the numerical models just after the application of the vertical stress, which is responsible for the decrease of the overall strength and stiffness, especially in the CDP model.

3.1.2. Deep repointing and injection method on masonry

The deep repointing method consists in a deep skiving of masonry lime mortar joints, making use of unporous cement mortar. The purpose of this methodology is to improve confinement in the masonry panels, increasing shear strength.

Obviously this restoration technique is suitable when clay bricks are well preserved while mortar presents degradation in the bonding properties.

This latter condition is exactly the situation observed on the rubbles of both towers: no significant damage is seen in the collapsed bricks, which exhibit an excellent level of conservation.

Injection consists in filling with cement mortar the cracked parts of the masonry walls. The goal is to restore consistency and internal continuity of the degraded material [19–22].

This kind of procedure is ideal for the consolidation of a masonry structure characterized by degradation and disruption which involves diffused cracks and empty parts [19–25].

This method requires, in order to be applied, that the injected mortar can penetrate the cracks and can diffuse along the whole extension of the discontinuity. It is commonly used in the case of historical buildings where the primary aim is to maintain the original appearance of the structure.

The combined effects of these two techniques have been tested in an experimental campaign led by Corradi et al. [25] on masonry panels extracted from different buildings. These samples were tested both before and after the repair intervention, to get an experimental evaluation of the increase in the strength and stiffness mechanical parameters, both in shear and compression.

As in the previous case, also for injection the choice of the binder is of primary importance: cement or lime mortar can be prescribed depending on the required strength increase. Otherwise, synthetic resins can be chosen, which are more fluid and easier to penetrate into the cracks. The limit of this technique is given by the difference in the deformability of the two bounded materials. Sliding effects and internal tension stresses due to shrinkage can occur between the injected material and the pre-existing structure causing dangerous instability phenomena. Certainly the restoration compatibility is questionable and raises doubts about the applicability in these specific cases.

In operational terms, it can also be stated that in our specific case the recourse to repointing and injection is improper, in view of the need to totally reconstruct the towers from the base.

Therefore, it makes more sense aiming for a solution where the internal layers consist of a masonry material with injections plus deep repointing with cement mortar, while the external leafs are made by lime mortar, in order to maintain the visual architectural compatibility required by the Ministry for the Cultural Heritage. According to data reported in Corradi et al. [25], in the numerical models it is assumed that deep repointing is done by removing 80 mm of lime mortar and substituting it with a more resistant one, with compression and tensile strengths of 10.75 MPa and 3.55 MPa, respectively. A cement mortar is used for injections, characterized by a 7 MPa compression strength and a 3 MPa tension strength. The value of the Young modulus is 8000 MPa.

On the basis of considerations based on the mixing rule, it can be stated that, in the numerical models referred to the improved material (by injections combined with deep repointing), the following mechanical properties should be assumed: +30% in terms of compression strength, shear resistance increased by a 2.5 factor and elastic stiffness increased by a 3.0 factor.

It is important to underline that the strength increase is associated to a stiffness increase and this is not necessarily beneficial in relation to the seismic behavior, because a stiffer structure is more stressed.

Applying the increasing factors, the mechanical parameters of the historical structures assume the values reported in Table 1.

As it can be seen from a comparison with the properties adopted for the original masonry, the friction angle remains essentially unchanged.

Table 1
Mechanical properties adopted in case of a reconstruction done with cement mortar.

ρ [kg/m^3]	E [MPa]	σ_c [MPa]	σ_t [MPa]	c [MPa]	φ [°]
1580	4500	3.12	0.50	0.375	30

Table 2
Synopsis of the mechanical properties adopted in the non-linear analyses.

	Historical masonry	Restored masonry	Injection and deep repointing	
ρ	1580	1710	1580	kg/m^3
E	1500	1491	4500	MPa
σ_c	2.4	6.2	3.12	MPa
σ_t	0.2	0.63	0.5	MPa
c	0.15	0.33	0.375	MPa
φ	30	33.6	30	°

To summarize, elastic and inelastic material properties used in the computations for historical masonry, restored masonry and deep repointing with injection are synoptically shown in Table 2. It is important to point out that the properties employed in the numerical analyses correspond to equivalent properties of a mortar-brick composite.

4. Numerical models of the towers

A detailed geometric characterization of both the towers based on the existing documentation made available by the Municipality of Finale Emilia and the Ministry for the Cultural Heritage (MiBAC), along with a wide photographic documentation collected by the authors, allowed the definition of detailed 3D geometric models of the towers.

The geometric models, entirely built within Rhinoceros system [26], have been imported and assembled into the ABAQUS Finite Element system. These models are discussed in [27].

Comparing numerical models to real structures shows that some simplifications have been introduced, in view of dealing with models which are simpler from the computational point of view.

For this reason, some details have been omitted; the spire and the belfry, for instance, have not been modeled, due to the secondary structural function. In this way, simplified yet realistic FE models have been built. Neglected details have been included in the structural analyses through the consideration of the corre-sponding mass.

Eight node brick elements have been used. The two FE models include 47,022 elements and 69,727 nodes (Clock Tower) and 39,695 elements and 60,061 nodes (the Fortified Tower of the castle).

Fig. 8 shows, for each structure, both the geometric model and the corresponding FE mesh.

4.1. Modal analysis

Eigen-values, eigen-modes and the corresponding effective mass are the preliminary output from the modal analysis, also useful to determine, despite not explicitly required by the Italian Code for the cases under study, the shape of the horizontal load distribution to be used within the static analysis and the pushover procedure.

Modal shapes for the first six natural modes corresponding to the analyzed cases, are shown in Figs. 9 and 10 for the Clock and Fortified Towers respectively. Table 3 lists periods, frequencies and effective masses in the X, Y and Z directions. Results correspond to classic expectations for masonry towers and might also be predicted with sufficient accuracy by means of simple beam models.

With reference to the historical material assumptions, the largest effective masses in the X and Y directions correspond to the first and second mode respectively and approximately represent 45% of the total mass. It is not surprising that a similar behavior is present along both the X and Y directions, in relation to the quasi square planar section of the structures. Small differences depend on some minor geometric irregularities (as openings) and the internal vault distribution.

With respect to the effective mass values, the same situation can be seen for the other material assumptions, and also for the Fortified Tower. This latter is characterized by a higher value of the effective mass percentage due to the value of the tower height.

From the comparison of period values it can be seen that, for both structures, the deep repointing with injection results into a period decrease. As expected, this is due to the stiffness increase. It is worth noting that in deep repointing with injection an increase of material resistance is also obtained, but the higher stiffness is generally associated to a stress increase when dealing with nonlinear static analyses. It is therefore interesting to understand if the strength increase is sufficient to secure an increase of seismic safety with the higher stress state induced.

The reconstituted masonry, on the contrary, exhibits a stable behavior in terms of both periods and effective masses, because of the negligible change in stiffness with respect to the unstrengthened case.

4.2. Equivalent static analysis under horizontal loads

The Italian guidelines for the built heritage [28] allow for a simplified evaluation of the seismic vulnerability of towers by means of equilibrium considerations.

It is worth noting that the equivalent static analyses are clearly independent from the inelastic material properties discussed previously, and also the elastic modulus is needed only in full 3D FE computations (if the cantilever beam hypothesis is done, even the elastic modulus is unnecessary).

The tower is modelled as a cantilever beam with variable stiffness and continuous mass distribution (depending on the irregularities, such as openings, vaults, wall thickness change, etc.) and the acting and resisting bending moments are compared along the structure geometric axis.

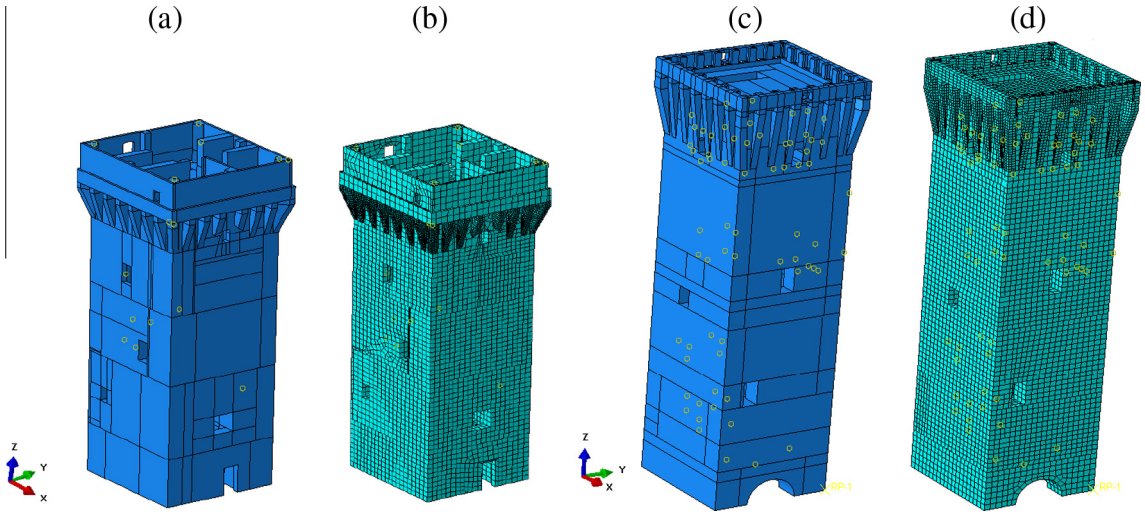

Fig. 8. Numerical models of the Clock Tower (a-b) and the Fortified Tower of the castle (c-d).

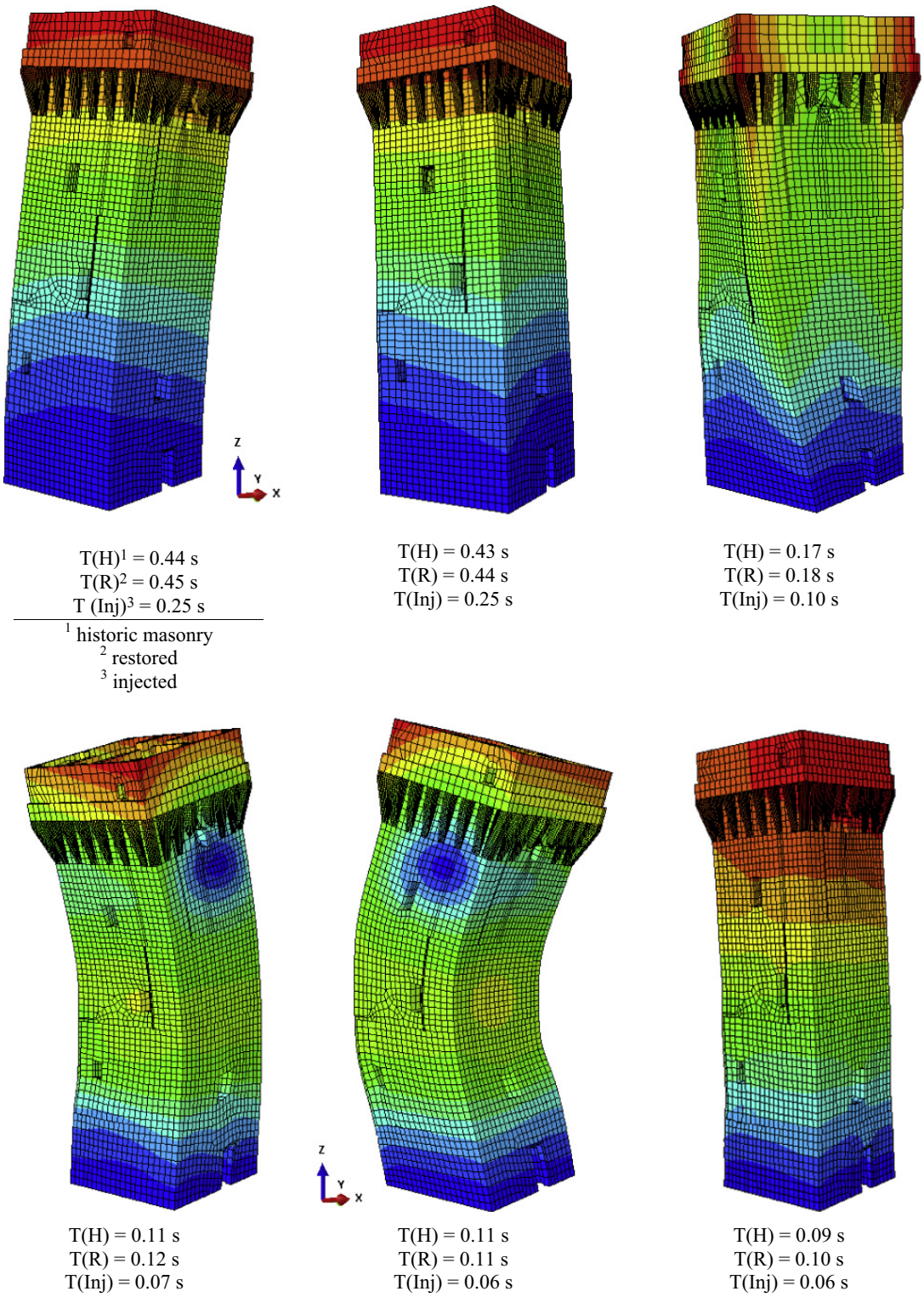

Fig. 9. Modal shapes for the Clock Tower (H = historical, R = restored, Inj = injected).

In order to evaluate the resisting bending moment, zero tensile stresses and a limited compressive strength are assumed for masonry.

For the problem at hand, the seismic action is characterized by a return period of 949 years and a D type soil is assumed. The corresponding response spectrum well approximates the real one, recorded during the May 20th earthquake. The response spectrum corresponding to a 475 years return period is also considered, to the purpose of a comparison with the action usually considered in structural design.

The q factor suggested by the Italian Code for such a type of structure is 2.8 and the adopted knowledge levels are the lowest (LC1) for historical masonry and the highest (LC3) in the other cases.

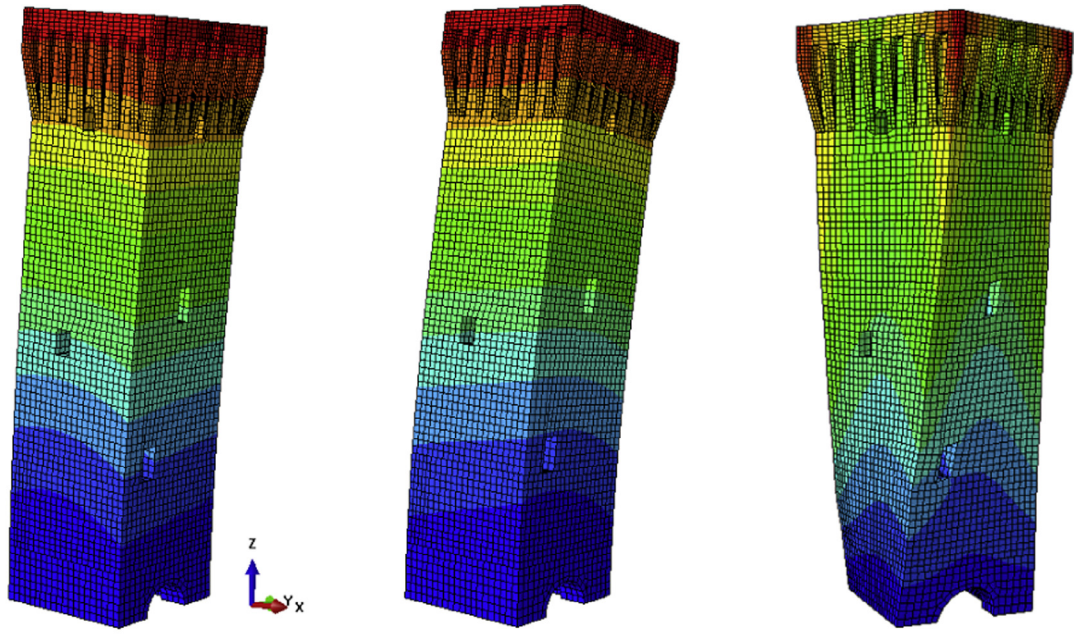

T(H) = 0.71 s
T(R) = 0.81 s
T(Inj) = 0.41 s

T(H) = 0.69 s
T(R) = 0.78 s
T(Inj) =0.40 s

T(H) = 0.22 s
T(R) = 0.25 s
T(Inj) = 0.13 s

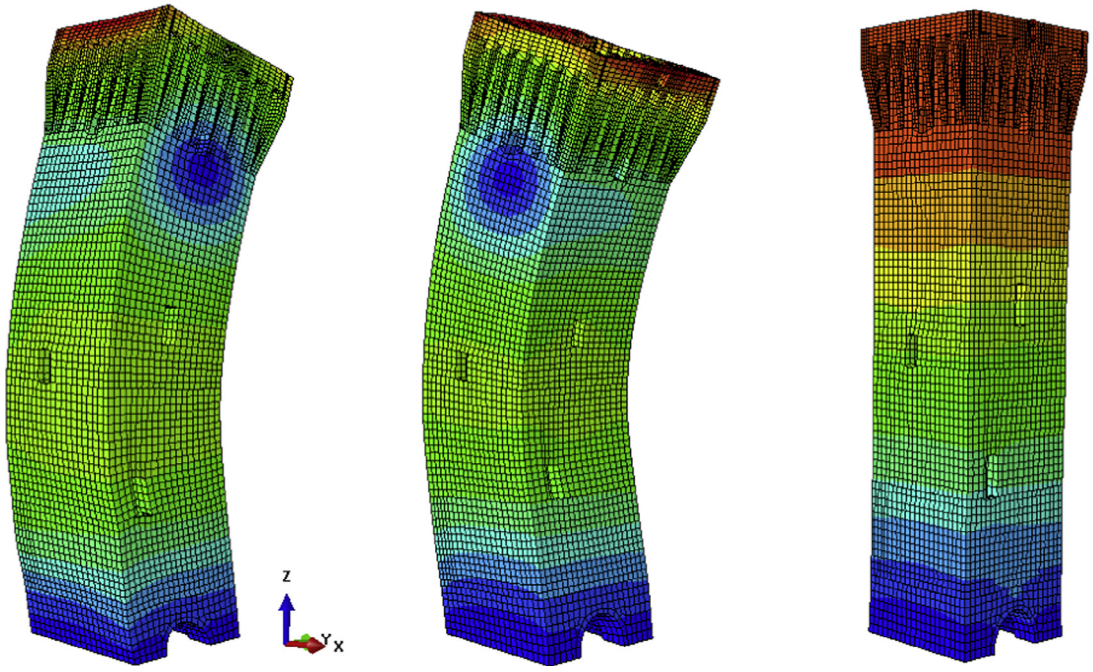

T(H) = 0.16 s
T(R) = 0.19 s
T(Inj) = 0.10 s

T(H) = 0.15 s
T(R) = 0.17 s
T(Inj) = 0.09 s

T(H) = 0.13 s
T(R) = 0.14 s
T(Inj) = 0.07 s

Fig. 10. Modal shapes for the Fortified Tower (H = historical, R = restored, Inj = injected).

The simplified structural assessment consists in the comparison between the acting and resisting bending moments at some cross sections along the height of the towers, for both principal inertia directions.

For towers with rectangular section, according to Italian Guidelines, simplified formulas can be adopted. Under the assumption that the normal compression does not exceed $0.85 f_d A_s$, the ultimate bending moment at any cross section can be evaluated as:

$$M_u = \frac{\sigma_0 A}{2}\left(b - \frac{\sigma_0 A}{0.85 a f_d}\right) \tag{1}$$

where a indicates the section width, b the height, A the section area, $\sigma_0 = W/A$ the average compression stress (W: tower weight above the section considered) and f_d the design compression strength.

External moments, within a cantilever beam model (subdivided into n elements), may be evaluated at the generic section j as:

Table 3
Synopsis of the results from the modal analysis in the different cases.

Mode	Clock Tower					Fortified Tower				
	Frequency [Hz]	Period [s]	Effective mass			Frequency [Hz]	Period [s]	Effective mass		
			X [%]	Y [%]	Z [%]			X [%]	Y [%]	Z [%]
Historical masonry										
1	2.30	0.44	44.3%	17.6%	0.0%	1.29	0.71	54.1%	7.2%	0.0%
2	2.34	0.43	17.6%	45.6%	0.0%	1.33	0.69	7.2%	54.3%	0.0%
3	5.75	0.17	0.0%	0.1%	0.0%	4.15	0.22	0.0%	0.2%	0.0%
4	8.75	0.11	0.6%	19.8%	0.0%	5.62	0.16	0.1%	24.2%	0.0%
5	9.20	0.11	20.9%	0.8%	0.3%	6.03	0.15	22.4%	0.1%	0.0%
6	10.63	0.09	0.1%	0.0%	78.7%	7.29	0.13	0.0%	0.0%	79.5%
Total participating mass[a]			91.0%	91.0%	79.3%			90.8%	95.4%	79.6%
Restored masonry										
1	2.23	0.45	43.0%	17.1%	2.2	1.24	0.81	52.7%	6.8%	0.0%
2	2.26	0.44	17.2%	44.3%	2.3	1.29	0.78	6.8%	52.8%	0.0%
3	5.55	0.18	0.0%	0.1%	5.6	3.99	0.25	0.0%	0.1%	0.0%
4	8.45	0.12	0.6%	19.3%	8.5	5.42	0.19	0.2%	23.5%	0.0%
5	8.89	0.11	20.3%	0.8%	8.9	5.81	0.17	21.7%	0.2%	0.0%
6	10.27	0.10	0.1%	0.0%	10.3	7.03	0.14	0.0%	0.0%	77.3%
Total participation mass			88.3%	88.40%	77.0%			87.9%	92.6%	77.3%
Injection and deep repointing on masonry										
1	3.96	0.25	43.9%	18.1%	0.0%	2.22	0.41	53.4%	8.0%	0.0%
2	4.02	0.25	18.2%	45.2%	0.0%	2.29	0.40	8.0%	53.6%	0.0%
3	9.93	0.10	0.0%	0.1%	0.0%	7.15	0.13	0.0%	0.2%	0.0%
4	15.03	0.07	0.6%	19.7%	0.0%	9.59	0.10	0.1%	24.1%	0.0%
5	15.81	0.06	20.8%	0.8%	0.3%	10.33	0.09	22.4%	0.1%	0.0%
6	18.35	0.06	0.1%	0.0%	78.6%	12.55	0.07	0.0%	0.0%	79.4%
Total participation mass			90.8%	90.9%	79.6%			91.1%	95.1%	80.0%

[a] The total percentage refers to a summation over the first 20 modes.

$$M_j = F_e z_j$$
$$z_j = \frac{\sum_{i=1}^{j} z_i^2 W_i}{\sum_{k=1}^{n} z_k W_k} \quad (2)$$

with $F_e = 0.85 S_d(T_1) W/g$ (S_d indicates the acceleration spectrum value for T_1, the structure main period; g is the gravity acceleration).

Instead of the bending stiffness, which is automatically available when a FE model and the elastic modulus are at disposal, it is important to derive the bending strength, to compare with the acting bending at the different transversal sections. This is done using Italian code Eq. (1) which takes into account in a simplified but effective way the peculiarities of the cross section (such as openings, presence of internal walls, thickness changes, etc.). Authors experienced a quite good agreement (discrepancies lower than 10%) between results provided by (1) and those obtained with a 3D FE discretization of a 1 m high portion of the tower with the investigated cross section, assumed to behave as a material unable to withstand tensile stresses and with limited compression strength, subjected to a increasing bending at the free transversal edge, the base being fixed.

Results of the comparison between resisting and acting bending moments are summarized in Fig. 11. In the figure, squares, crosses, triangles and diamonds belonging to resisting bending moment curves along towers height represent the places where the transversal sections are considered to estimate the ultimate flexural strength. Respectively 10 and 12 transversal sections are considered for the clock and fortified tower. The positions where the cross section strength is evaluated are not equally stepped, but it was made the choice to investigate the flexural behavior at meaningful locations, to obtain results more representative of the tower real geometry, at the same time limiting the computational effort.

As it results from Fig. 11, in all cases the lower part of the structure exhibits insufficient strength against bending actions. Openings present in the tower lower part further weaken the transversal section, and reduce the corresponding resistance level. This is typical of the aforementioned simplified approach, which usually leads to the estimation of high vulnerability levels, associated to the formation of a flexural hinge at the base.

Such a failure mode appears the most critical for all the material assumptions and it is interesting to notice that the increase in the material strength is not sufficient to ensure structural safety, in particular in the case of the Fortified Tower which is characterized by a weak base section.

The cases shown in Fig. 11 refer to the historical masonry and the restored one only. The injected masonry case is not represented, providing results not significantly different from the case of restored masonry.

4.2.1. Evaluation of the seismic safety index and acceleration factor

The Italian Guidelines for the Architectural Heritage [28] recommend to perform the safety assessment by means of the so called vulnerability index I_s defined as follows:

$$I_{S,SLV} = \frac{T_{SLV}}{T_{R,SLV}} \quad (3)$$

where T_{SLV} is the earthquake return period associated to the ultimate limit state (life safeguard, SLV) for the examined structure and $T_{R,SLV}$ is the reference return period. Clearly an index greater than one corresponds to a safe state.

The seismic safety index I_S, being based on the return periods corresponding to both the seismic demand and the structural capacity, allows also for an evaluation of the structure in terms of limit return period.

The estimation of another index, called acceleration factor, is also required; this is defined as the ratio between the soil peak accelerations corresponding to structural capacity and demand:

$$f_{a,SLV} = \frac{a_{SLV}}{a_{g,SLV}} \quad (4)$$

where a_{SLV} is the soil acceleration leading to the SLV ultimate state and $a_{g,SLV}$ is the acceleration corresponding to the reference return

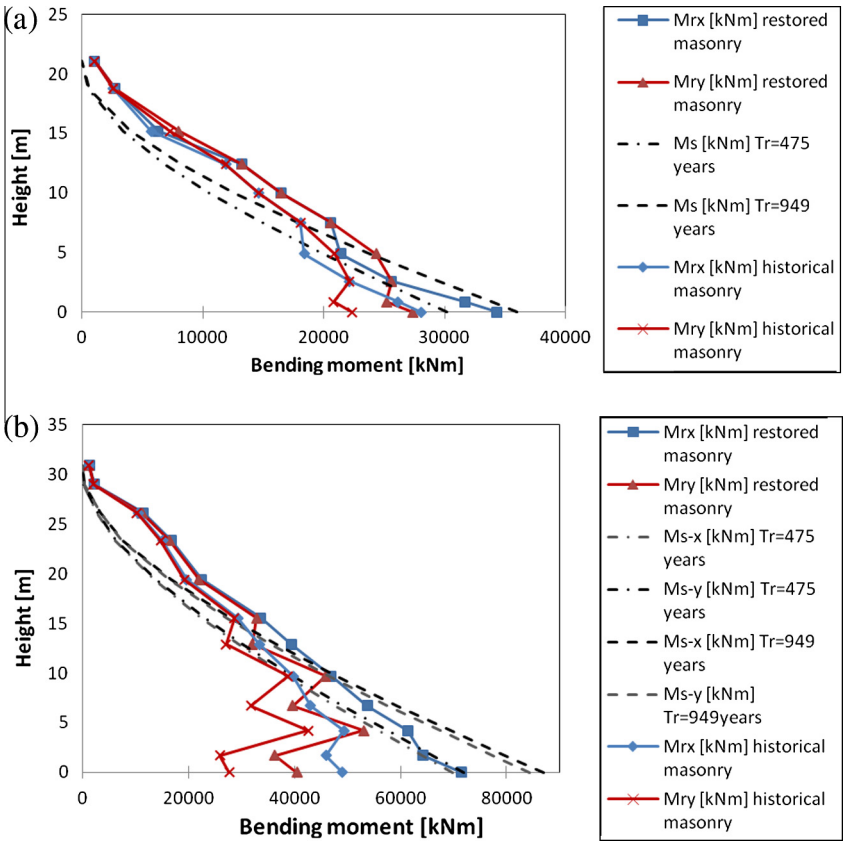

Fig. 11. Comparison between bending moment and resistant moment for the Clock Tower (a) and the Fortified Tower (b).

period. It is interesting to notice that this latter index is a purely mechanical parameter, which may be useful for an evaluation of the weakness of the structure in terms of strength.

In order to evaluate the response spectrum acceleration for which the SLV limit state is reached at the i-th section, the following equation is used:

$$S_{e,SLV,i}(T_1) = \frac{qgM_{R,i}\sum_{k=1}^{13} z_k W_k}{0.85WF_C\left(\sum_{k=i}^{13} z_k^2 W_k - z_i \sum_{k=i}^{13} z_k W_k\right)} \tag{5}$$

where q is the behavior factor, g the gravity acceleration, $M_{R,i}$ is the resisting moment at the i-th section, z_k and W_k are the height and the weight corresponding to of the k-th section (the total number of cross-sections is equal to 13 in that particular case), respectively, W the total weight, F_C the confidence factor and z_i the height of the i-th section from the base.

As the cross section where the minimum value of $S_{e,SLV}$ occurs has been identified, the return period T_{SLV} of the corresponding seismic action may be found by means of an iterative procedure with linear interpolation. This procedure is based on data available in the Italian Code - Appendix [2] which provides, at each point of the reference topographic grid, the spectral values (a_g, F_0 e T_c^*) for return periods of 30, 50, 72, 101, 140, 201, 475, 975 and 2475 years.

In the analyzed cases, the minimum spectral acceleration is associated to the base section.

Finally, in order to convert the minimum spectral acceleration into the corresponding soil acceleration, the following equation is used:

$$a_{SLV} = \begin{cases} \frac{S_{e,SLV}}{SF_0} & T_B \leqslant T_1 \leqslant T_C \\ \frac{S_{e,SLV}}{SF_0}\frac{T_1}{T_C} & T_C \leqslant T_1 \leqslant T_D \end{cases} \tag{6}$$

where T_B, T_C and T_D are the reference periods in the definition of the response spectrum according to the Italian Code and the S coefficient depends on the soil and topographical categories. The values of I_S and f_a evaluated for the case of the restored towers (it is worth noting that all hypotheses done provide similar results) are reported in Table 4.

As it can be seen, the safety index I_S is always much lower than 1, even in the presence of restoration works. For a soft soil (D type) the situation becomes critical, with an extremely low value of I_S (0.10) for the Fortified Tower. Both towers are slightly more vul-

Table 4
Evaluation of I_s and f_a indexes (bold numbers indicate insufficient safety) for the Clock Tower and the Fortified Tower.

X direction						Y direction					
$S_{e,slv}(T1)$ [g]	T_{slv}	$T_{R,Slv}$	I_s	a_{slv} [g]	f_a	$S_{e,slv}(T1)$ [g]	T_{slv}	$T_{R,Slv}$	I_s	a_{slv} [g]	f_a
Clock Tower											
0.707	505	949	***0.53***	0.166	***0.84***	0.563	312	949	***0.33***	0.132	***0.67***
Fortified Tower											
0.558	307	949	***0.32***	0.160	***0.81***	0.315	92	949	***0.10***	0.090	***0.45***

nerable along the Y direction, due to the openings present at the base along this direction.

Furthermore, it is worth underlining that the case corresponding to the maximum value for I_S (C type soil and seismic load along the X direction) is associated to a ground acceleration a_{SLV} equal to 0.093 g, much lower than the PGA registered during the 20th May shake (roughly equal to 0.25 g).

Finally, it should be noted that also for a lower seismic action, associated to a reference return period equal to 475 years, both towers are not in a safe condition, with minimum values of I_S equal to 0.66 and 0.19 for the Clock and the Fortified Tower, respectively, and f_a = 0.81 and 0.54. Along the X direction, in the latter case, the Clock Tower results in a safe condition, with I_S = 1.07 and f_a = 1.02.

4.3. 3D pushover analysis

The so-called pushover analysis is a non-linear static procedure generally used to determine the structural behavior against horizontal forces. It consists in a simplified procedure, which has been adopted in the last few years also for the non linear static analysis of masonry structures. Basically, a computational model of the structure is loaded with a proper distribution of horizontal static forces, which are gradually increased with the aim of "pushing" the structure into the nonlinear field. The resulting response (capacity curve) conveniently represents the envelope of all the possible structural responses, and can thus be used to replace full nonlinear dynamic analyses. In this work, full 3D pushover analy-ses have been performed on the previously described 3D models [29,30].

As required by the Italian Code, two different load conditions must be considered in the analysis, both depending on the mass distribution: in the G1 distribution, forces are directly proportional to the product of the height by the mass, while in G2 they are simply proportional to the mass. Analyses are performed along both the X and Y direction.

Pushover can be utilized within the so-called N2 method for a global check of the vulnerability of the structure. Such vulnerability is synthetically evaluated by means of a comparison between the displacement capacity d_c^* and the displacement demand d_d^* obtained by means of the pushover analysis, both referring to the same control point. The displacement capacity is evaluated with respect to an equivalent single degree-of-freedom system characterized by a bilinear behavior in a shear force-displacement diagram.

First, the pushover curve is scaled by means of the so called participation factor of the fundamental eigenvector $\Gamma = \frac{\sum m_i \Phi_i}{\sum m_i \Phi_i^2}$, where Φ_i is the i-th component of the eigenvector Φ and m_i is the mass of i-th node. The fundamental eigenvector Φ is deduced from standard FE modal analysis.

Assuming as F_b and d_c the actual base shear and corresponding displacement of the structure respectively, the scaled values are $F_b^* = F_b/\Gamma$ and $d_c^* = d_c/\Gamma$. Assuming as F_{bu} the peak base shear, then $F_{bu}^* = F_{bu}/\Gamma$.

Once found the pushover curve of the equivalent system $(d_c^* - F_b^*)$, it is reduced to a bilinear elastic perfectly plastic diagram, whose characteristics are defined by the elastic stiffness k^*, ultimate shear F_y^* and the ultimate displacement d_u^*. k^* is evaluated plotting the secant to the equivalent capacity curve at a shear force equal to the 70% of the maximum value F_y^*. The bilinear diagram is completed assuming an area equivalence between the equivalent and the bi-linear system, where the equivalent curve is stopped at a displacement d_u^* corresponding to a base shear equal to 85% of the peak shear.

The numerical analyses are conducted using an arc length routine, to deal with the possible softening in the global pushover curve, which is however hardily visible in such kind of structures. As explicitly suggested in Italian Guidelines for the Built Heritage, the utilization of materials without softening (like elastic-perfectly plastic models, an hypothesis which implies by definition to find global pushover curves without any softening) is admitted, both because of the extreme complexity in performing non-linear static analyses with 3D geometries and for the diffused unavailability of materials with softening within commonly used commercial codes. On the other hand, it should be pointed out that, even in the presence of softening for the material, this is uncommon in the global response. As known, ultimate capacity for masonry with low tensile strength is, indeed, trivially linked to vertical dead loads and the global contribution of fracture energy cumulated for cracks forming in tension is reasonably negligible. That's one of the reasons why limit analysis computations are preferable in such cases, as stated for example in [23,24]: they are reliable and require a fraction of the time needed by standard FEM. In the absence of any clear softening, the key question is therefore to identify the correct displacement of the control node for which the numerical analysis should be stopped. In [28] considering the difficulties in the definition of the displacement at the ultimate limit state, it is recommended to evaluate the ratio between the elastic limit base shear and the ultimate shear of the bi-linear system. Such a ratio cannot exceed a maximum admissible value, defined on the basis of the ductility and dynamic features of each construction typology, and in any case ranging between 3 and 6. Typically the aforementioned procedure is iterative, but requires a short time for a robust convergence. In case of masonry towers, which behave roughly as cantilever elasto-plastic beams (with plastic flexural hinge forming near the base), the ratio between ultimate and elastic limit load does not exceed 2, depending strongly on the shape of the transversal section. For hollow sections with thin walls, the ratio can further reduce to less than 1.5. Such characteristic outcome is experienced also for the cases at hand, where quite flat pushover curves are obtained, see Fig. 12. On such a basis, the lower bound suggested by the Italian code is further reduced to 1.8 for the sake of safety, and elastic and ultimate displacement limits indicated in Fig. 12 with a circle and a square respectively are obtained iteratively.

The ultimate SDOF equivalent system base shear F_y^*, in the absence of a clear global softening, is assumed equal to F_{bu}^*.

The elastic period of the bilinear system is $T^* = 2\pi\sqrt{m^*/k^*}$ where m* is the equivalent mass and $k^* = F_y^*/d_y^*$.

The ductility of the normalized capacity curve is defined as the ratio between the ultimate and the yield displacement, i.e. $\mu = d_u^*/d_y^*$.

Finally, the Italian code allows the estimation of the displacement demand $d_{\max}^*$ using the elastic displacement spectrum

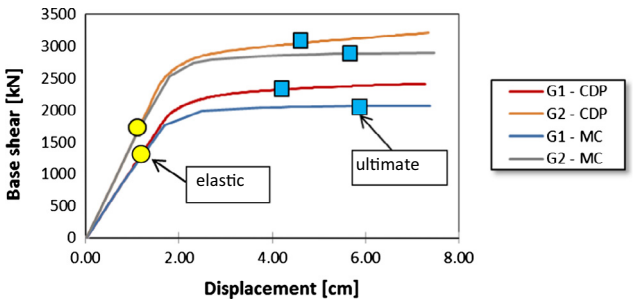

Fig. 12. Comparison of capacity curves corresponding to different constitutive laws, with reference to some computational results found for the Clock Tower.

$S_{De}(T^*)$. The base shear corresponding to d^*_{max} on the elastic one DOF system is F^*_e.

Once known d^*_{max}, it has to be checked if $d^*_{max} \leqslant d^*_u$. This check can be done either analytically or graphically, using the so-called N2 method. For masonry, the Italian code requires also that the ratio q^* between the base shear evaluated using the elastic spectrum F^*_e and the equivalent 1 DOF system F^*_y does not exceed 3.

The aim is therefore synthetically to verify if the capacity of the structure in terms of maximum displacement is sufficient to satisfy the demand, in relation to the spectral action considered.

Preliminarily, to the purpose of verifying the reliability of the calibration procedure done on the material, a comparison between the capacity curves obtained for the Clock Tower assuming for masonry the two constitutive relationships considered in the previous Section (MC and CDP) is done; results are shown in Fig. 12.

Similar results are obtained for the Fortified Tower, but the results are left out for the sake of conciseness. As it can be seen, the agreement is satisfactory from an engineering standpoint, meaning that the MC approximation, which is computationally less demanding, can be adopted to perform sensitivity analyses on material properties for a reliable investigatation of the structural behavior in the non-linear static range.

4.3.1. Sensitivity analysis

Before analyzing the structural behavior in relation to the different material assumptions, a sensitivity analysis is performed to understand the seismic performance of the towers under the effect of static horizontal loads varying Mohr-Coulomb strength domain parameters over a wide range. An elastic-perfectly plastic behavior with associated flow rule is adopted for the material.

It is worth noting that a Mohr-Coulomb model well adapts to repeated computation within sensitivity analyses, because the inelastic behavior depends exclusively on two mechanical parameters, namely cohesion and friction angle, defining the strength domain. Conversely, any more complex approach, like either a concrete damage-plasticity CDP or a smeared crack model requires setting a variety of inelastic material constants, especially to properly describe softening and non-linear strain evolution, both in tension and compression.

In addition, it should be pointed out that, when dealing with pushover analyses on masonry towers, global softening is rarely experienced, because masonry behaves as a quasi no-tension material and great part of the non-linear behavior is ruled by the structure weight. As a consequence and as also highlighted explicitly by Italian Guidelines on Architectural Heritage [28], an elastic-perfectly plastic approach may be fairly representative of the actual behavior.

Finally, it should be remarked that uncertainty in material parameters determination for such kind of structures is a key issue that, however, would require dedicated sophisticated computations based on large scale Monte Carlo simulations, where masonry mechanical properties are spatially varied at random, assuming a certain statistical distribution for the parameters defining the inelastic behavior. Sensitivity analyses are thought as a very preliminary step to deal with material uncertainties, which however remain extremely demanding for 3D FE models with sophisticated non-linear materials and many FEs.

Here, cohesion values of 0.15, 0.20 and 0.30 MPa and friction angles of 25°, 30° and 35° are permutated in the pushover analyses, and the value of the ultimate displacement for the control node is assumed as output variable.

Results are shown in Figs. 13 and 14 for the Clock and Fortified Tower, respectively.

As can be clearly noticed, the Clock Tower is characterized by a linear variation of the ultimate displacement varying cohesion and friction angle. This means that the failure mechanism does not change considerably when material properties are varied. This mechanism is characterized by an inclined crack surface forming near the base, with inelastic deformations due to combined shear and bending actions, see Fig. 15a where the equivalent plastic strain patch at failure is shown.

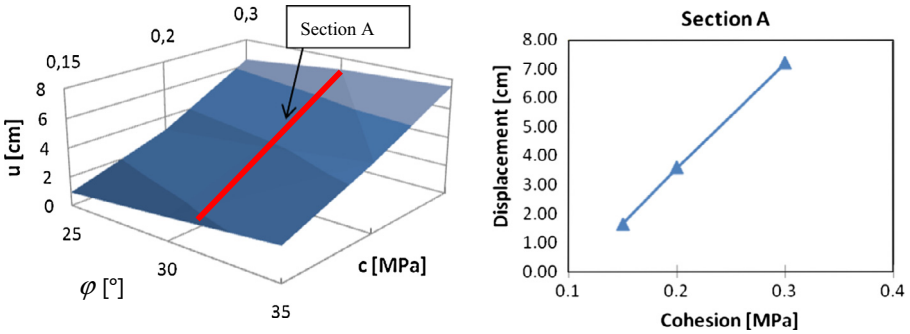

Fig. 13. Clock Tower, ultimate displacement of the control point varying MC cohesion and friction angle values.

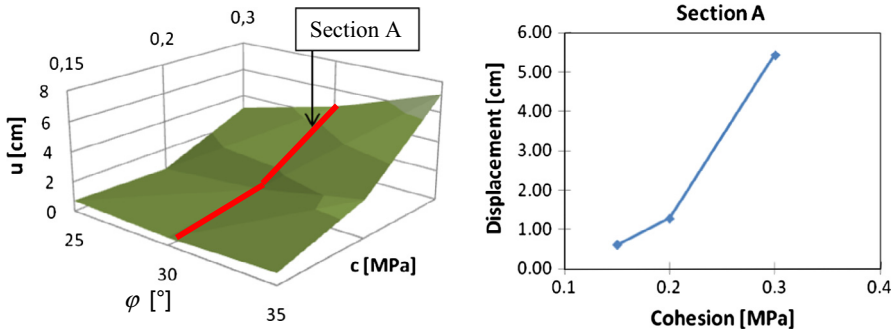

Fig. 14. Fortified Tower, ultimate displacement of the control point varying MC cohesion and friction angle values.

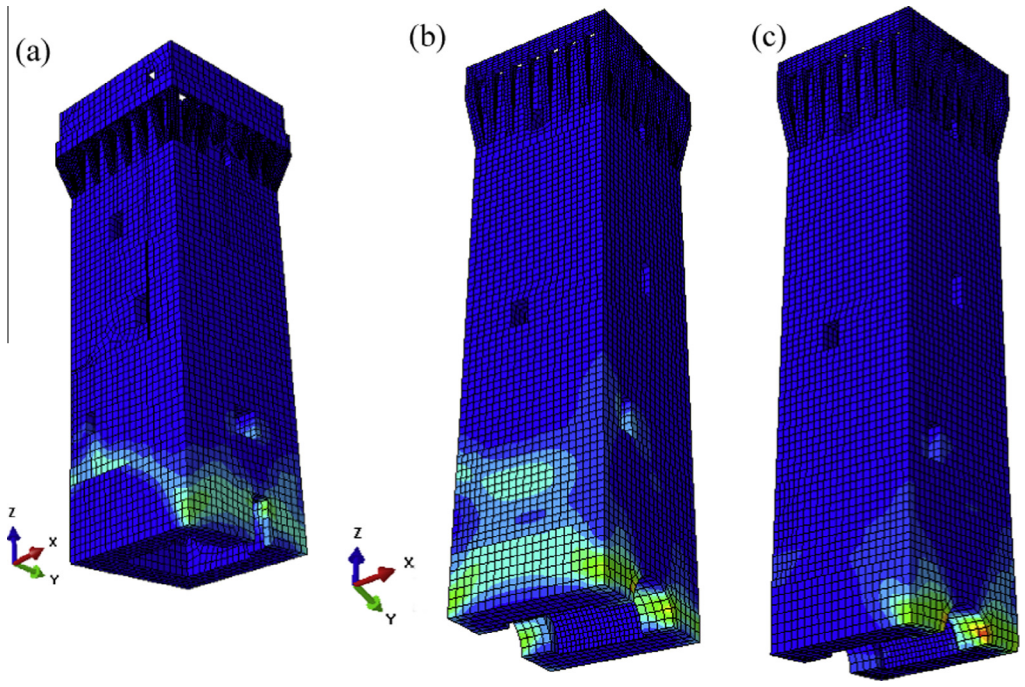

Fig. 15. Plastic strain distribution at the end of the pushover analysis for the Clock Tower (a) and for the Fortified Tower with two different levels of masonry resistance (b)-(c).

The behavior of the Fortified Tower is different, exhibiting a non linear dependence of the ultimate displacement on the c and Φ parameters, see Fig. 14, which suggests the activation of a different failure mechanism. Such a conclusion is confirmed by the inelastic deformation patches shown in Figs. 15-b and c. For small cohesion values, failure is mainly characterized by the limited shear strength of the materials, with formation of diagonal cracks near the base. As cohesion increases, the failure mechanism exhibits a typical flexural hinge at the base cross section, which indeed is weakened by the arch openings. As expected, the role played by the friction angle in the modification of the failure mechanism is secondary, as indicated by the shape of the ultimate displacement surface shown in Fig. 14.

4.3.2. Safety assessment through the pushover analysis

Previous sensitivity analyses have provided general information about the dependence of the seismic response on the material mechanical properties.

As it usually occurs for such kind of structures, the G1 distribution of loads is always more critical; in the following, therefore, we will refer exclusively to this load case.

The seismic action considered in the safety assessment is the one provided by the Italian Code, which well approximates the real action recorded on May 20th, characterized by a return period of 949 years.

On the basis of 3D nonlinear analyses, seismic vulnerability is evaluated, as already pointed out, comparing the displacement capacity $\boldsymbol{d}_{\boldsymbol{c}}^{*}$ and the displacement demand $\boldsymbol{d}_{\boldsymbol{d}}^{*}$. As it usually occurs for towers, control points have been selected on the top cross-section, in the middle of one of the edges.

The pushover curve is scaled by means of the participation factor Γ, as discussed extensively in the previous Section. The scaled values for base shear and displacement are $F_b^* = F_b/\Gamma$ and $d_c^* = d_c/\Gamma$, respectively.

According to the Italian Code, the bilinear curve is obtained imposing the geometric conditions already illustrated in the previous Section, where the reader is referred for further details. The ductility of the bilinear curve is defined as the ratio between the ultimate and the yield displacement: $\mu = d_u^*/d_y^*$.

With reference to T^*, the displacement demand $d_{\max}^*$ is evaluated through the elastic displacement response spectrum $S_{De}(T)$.

Fig. 16 shows the graphical representation of the N2 method in the AD (acceleration-displacement) plane for the pushover analyses relative to both towers in all the considered cases.

As it can be noted, historical masonry exhibits a poor performance for both towers. In agreement with the real situation, pushover analyses confirm the high seismic vulnerability level and, implicitly, the collapses occurred.

Different results are found for restored masonry: recovering the original material resistance (in particular for mortar) looks sufficient to avoid the collapse of both structures.

An interesting result, somewhat in contrast with intuition, can be finally observed with reference to injected masonry. This strengthening procedure (in combination with deep repointing), in terms of maximum strength, provides results similar to those found for restored masonry, but also associated to a large stiffness increase. This last feature is not beneficial in terms of N2 safety assessment, as shown in Fig. 16, where it is clearly indicated that a border line situation is obtained by means of such a restoration intervention, especially for the Fortified Tower. A synopsis between resultant displacement capacity and demand is reported in Table 5.

4.4. Non-linear dynamic analysis

To the purpose of an accurate interpretation of the effects induced by the May 20th seismic event in terms of cumulated damage/activation of failure mechanisms and to realistically predict what would have happened if suitable consolidation procedures were realized prior the earthquake, full 3D non-linear dynamic analyses have been performed.

A real accelerogram, recorded during the May 20th shake in Mirandola, has been applied at the base along the three principal inertia directions, see Fig. 3.

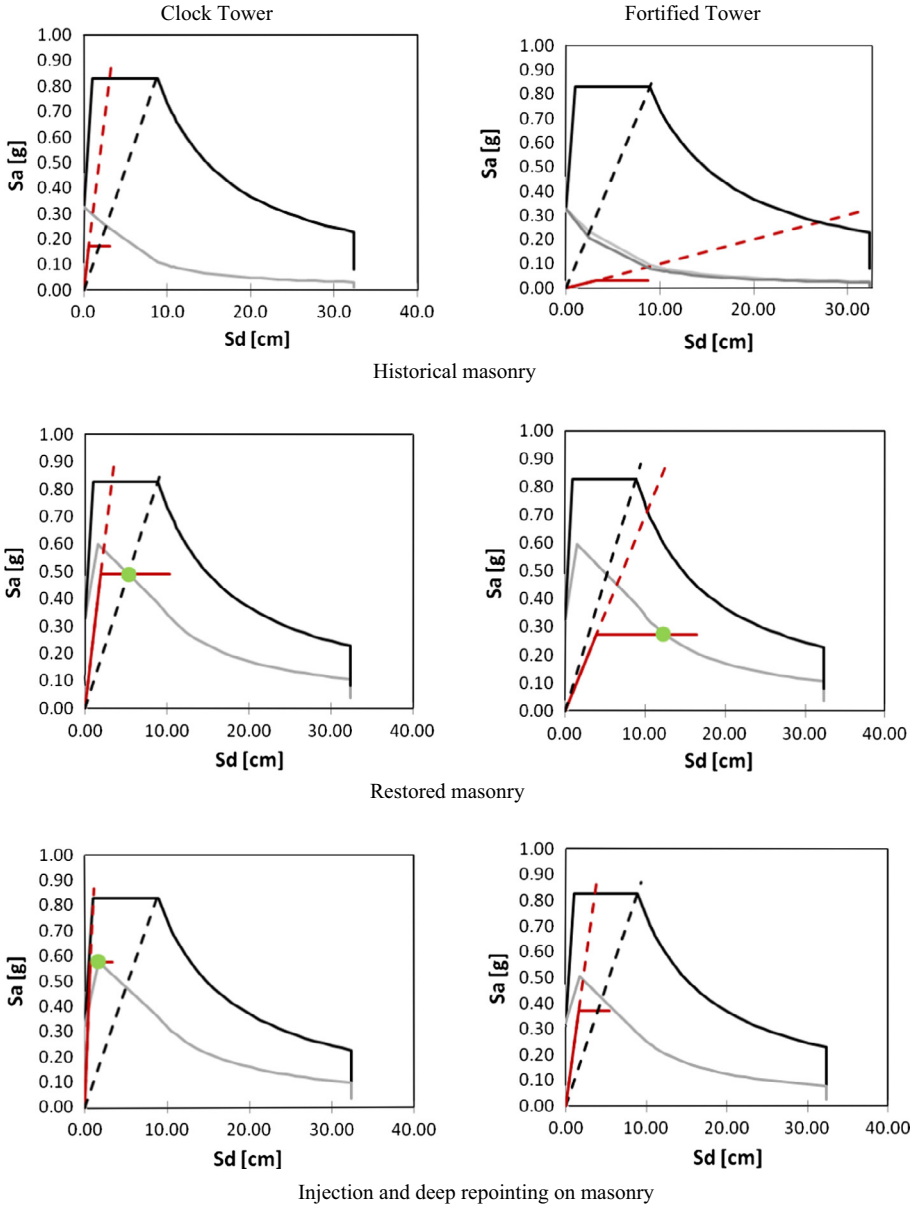

Fig. 16. Results of N2 safety assessment.

Table 5
Comparison between displacement capacity and demand obtained applying the N2 method in the various restoration cases.

	Clock Tower		Fortified Tower			
	G1x		G1x		G1y	
	d_{max} [cm]	d_u[cm]	d_{max}[cm]	d_u[cm]	d_{max}[cm]	d_u[cm]
Historical masonry	7.94	4.68	17.03	13.30	16.06	11.22
Restored masonry	8.13	15.73	18.74	31.32	15.12	32.51
Injected masonry	2.42	5.04	9.18	8.23	8.60	9.76

Both material and geometrical non linearity has been considered in the analyses. The same CDP model used for the pushover analyses is here employed, because it is crucial to reproduce not only the stiffness and strength deterioration but also the dissipative characteristics associated to the cyclic hysteretic behavior and the damage development during the event.

After studying the real situation with the application of X,Y and Z accelerogram components, a further analysis has been performed by removing the Z component, with the aim of understanding the importance of the vertical acceleration on damage propagation. Authors experienced very similar results, probably because of the reduced slenderness of both towers.

4.4.1. Clock Tower

From the tensile damage patch registered at the end of the simulations of May 20th shake (20 s), see Fig. 17, it can been seen that

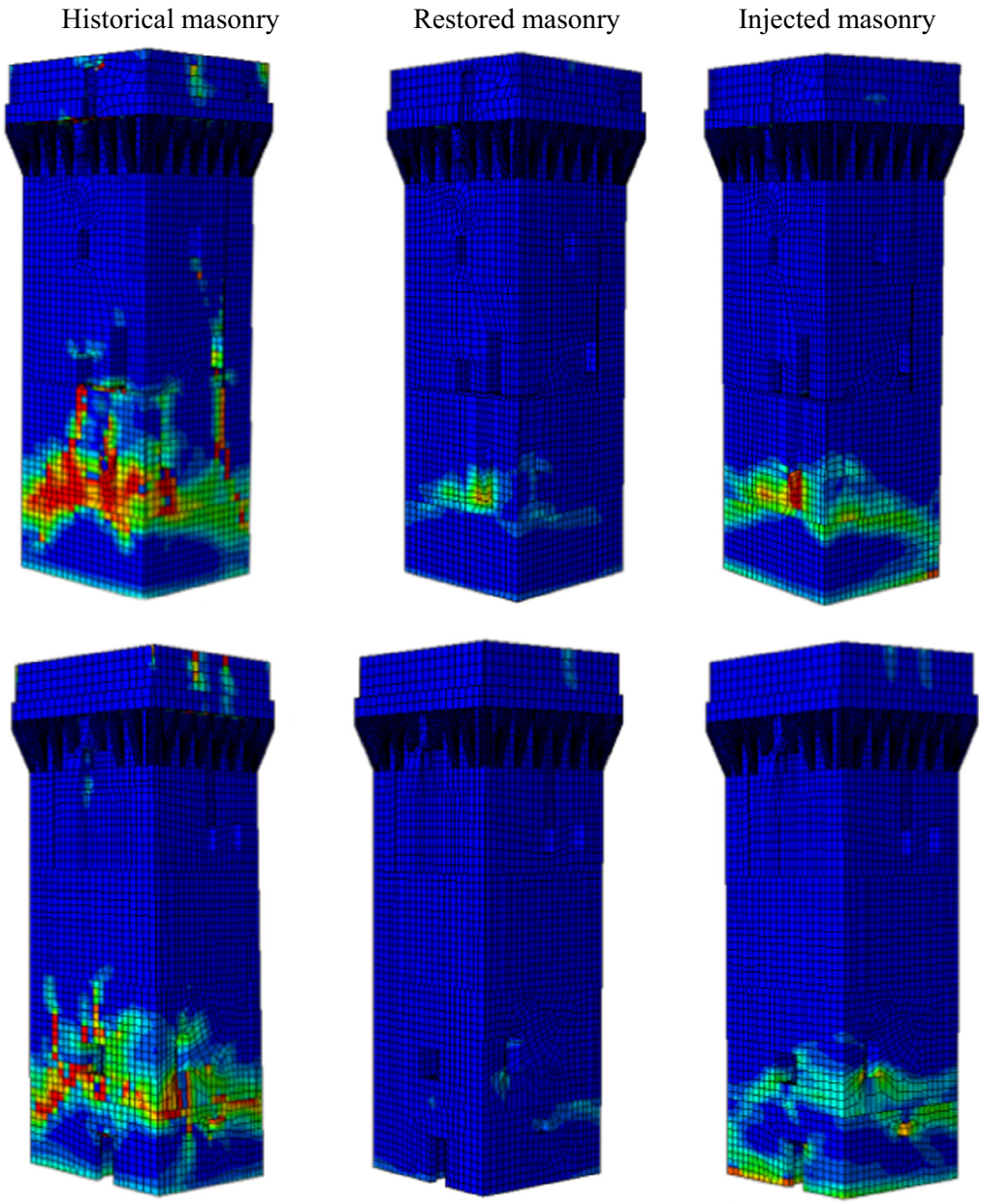

Fig. 17. Clock Tower, tension damage distribution. Top: S-W view. Bottom: N-E view.

the structure suffered from the formation of several cracks. Damage spreads along an almost horizontal plane near the base and proceeds vertically, in correspondence of the openings up to about the tower mid-height.

In particular, vertical cracking propagation near the openings fairly corresponds to what really happened, before the total collapse of the structure, see Fig. 2. While some differences between these damage maps and those found in non-linear static analyses are evident, the dynamic behavior of the tower has some clear similarities with that occurred in reality, such as the formation of a mixed shear and flexural hinge near the first floor level. This is not surprising, since it is largely demonstrated that static incremental analyses, following the first mode deformation scheme, may not reproduce realistically the failure mechanism induced by a dynamic analysis, which, on the contrary, takes into account the contribution of higher modes, which may become important to reproduce the effective collapse mechanism, as observed in the reality.

Fig. 18 shows also the displacement variation in both the north-south and east-west directions, measured at the top of the tower as a function of time. At the end of the seismic excitation a residual displacement of about 4 cm along the east-west direction once more emphasizes that two tower sides suffered more damage.

The results corresponding to the case of restored masonry show a different situation, with a reduction in the damage spread by the geometrical discontinuities, where stress concentration is likely to occur. The amount of damage and the residual displacement relative to a control node at the tower top, see Fig. 18, allow to conclude that the collapse state is far to occur, meaning that this restoration intervention is very effective in terms of vulnerability reduction.

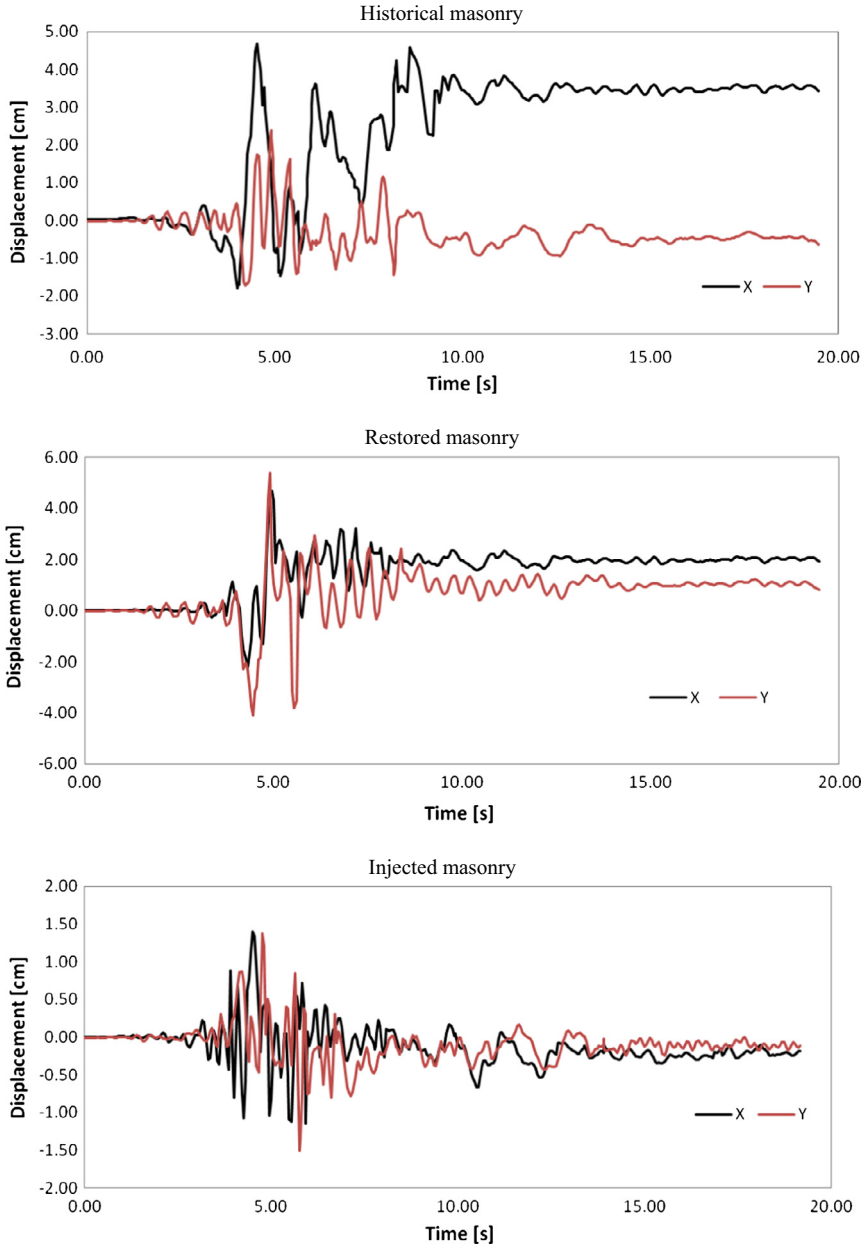

Fig. 18. Relative top section displacement of the Clock Tower during the May 20th seismic event.

Finally, the deep repointing technique associated to injections provides an intermediate behavior between the previous ones, where damage is mainly concentrated at the base, not as widespread as for the historical masonry case. Having also a look into the residual displacements of the control node, Fig. 18, a safe situation comes out again, even if the damage distribution is much higher than in the case of traditional restoring. The more pronounced damage distribution is connected to stiffness increase, as described in the material consolidation results.

4.4.2. Fortified Tower

The same kind of analyses, when performed on the Fortified Tower, again show how the application of the real accelerogram is critical in the case of historical masonry, i.e., when poor mechanical properties are assumed for masonry. The greater height of the Fortified Tower with respect to the Clock Tower results into a worse situation.

The cumulated tension damage patch at the end of the simulations, see Fig. 19, shows the activation of a combined shear-flexural hinge near the base, with diagonal cracks spreading upwards. This is probably the real failure mechanism which was activated during 20th May first shake, even if a precise photographic documentation is missing. From what reported by direct observers (the shake occurred night time), it seems that the tower suffered a failure at the first floor level, with the overturning of the upper part and, subsequently, the total failure of the tower, collapsing against the castle wall.

The residual displacement of the control node, located at the top, see Fig. 20, is greater than for the Clock Tower, because of the different height, and compatible with the activation of a failure mechanism.

After a hypothetical restoration procedure based on traditional techniques, the tower would undergo a situation of quasi total absence of damage, similarly to what found for the Clock Tower

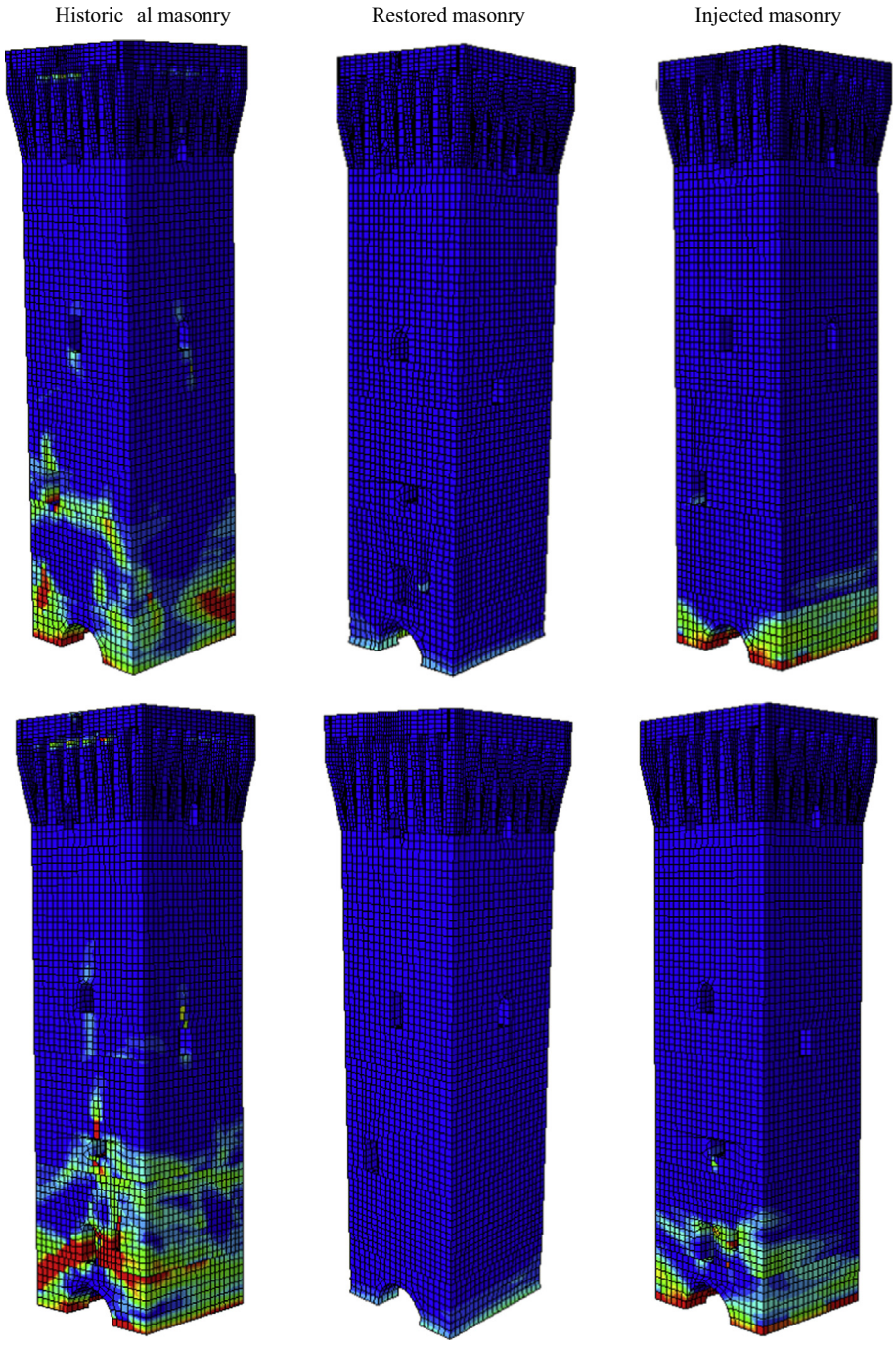

Fig. 19. Fortified Tower, tension damage distribution. Top: N-E view. Bottom: S-W view.

see Fig. 19. The residual displacement is minimal (2 cm), because of the negligible cumulated damage, Fig. 20.

An interesting result is finally worth noting with reference to injected masonry. In partial agreement with the results found in the pushover analyses, the increased stiffness results into more damage than in the previous case, with a clear formation of a flexural hinge at the base of the structure, see Fig. 19. The residual displacement at the end of numerical simulations, Fig. 20, looks too small to suggest the full activation of a failure mechanism, but highlights that the use of cement mortar for the tower reconstruction is not recommended and that traditional techniques are preferable.

6. Conclusions

In the paper, a wide numerical investigation into the seismic behavior of two masonry towers (the Clock and Fortified Towers in Finale Emilia, both collapsed during the 2012 Emilia earthquake) has been presented.

Three assumptions on the mechanical properties of the masonry material are analyzed in detail, with the aim of investigating the structural performance (1) in a situation similar to the real one at the time when the seismic event occurred and (2) after two hypothetical rehabilitation interventions executed before the seismic event, based on either traditional materials (lime mortar) or

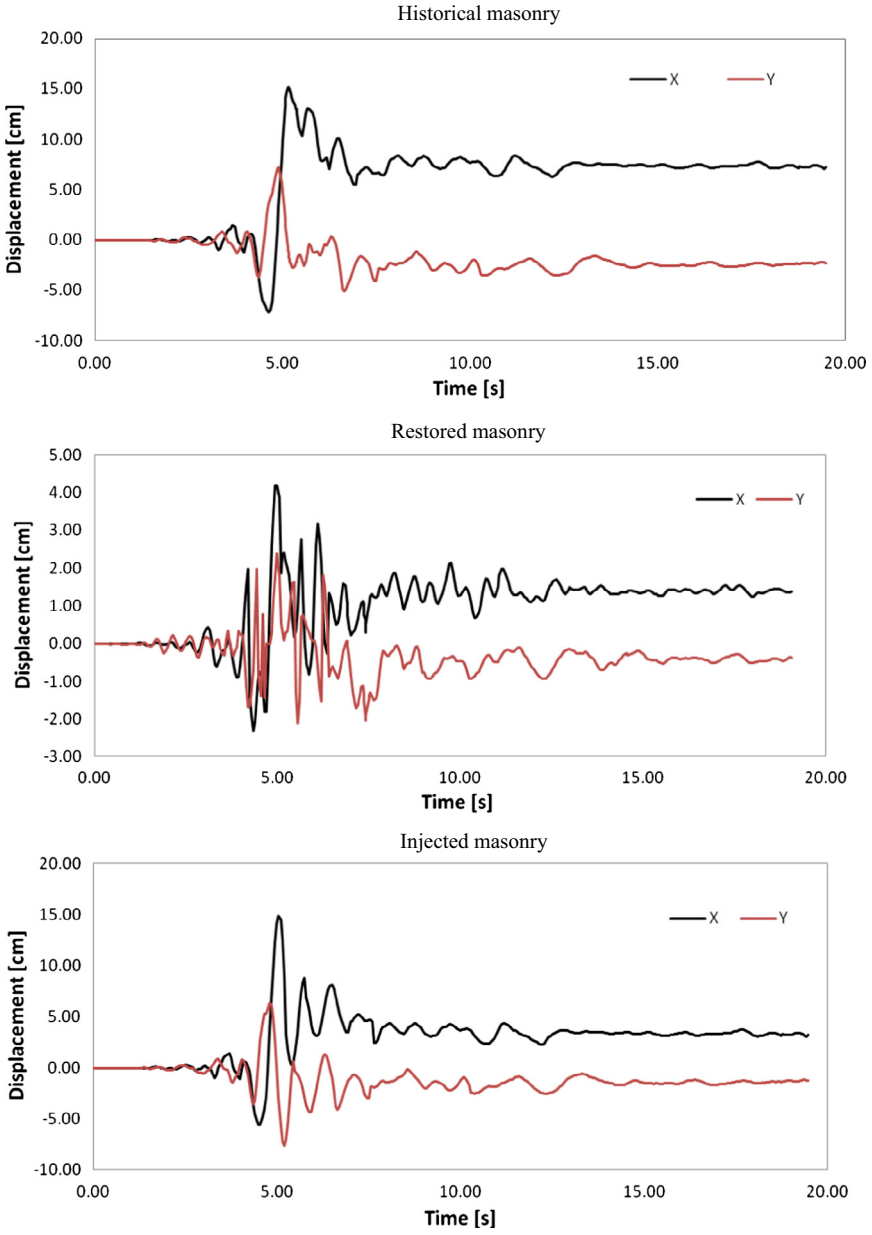

Fig. 20. Relative top section displacement of the Fortified Tower during the May 20th seismic event.

deep repointing plus injections with cement mortar. The seismic upgrading options are analyzed in detail, not only because they could have drastically changed the seismic performance of both towers, partially preserving their integrity and precluding the total collapse, but also because they provide useful hints for future reconstruction interventions aiming at a situation of lower seismic vulnerability.

The employed numerical procedures include modal analyses, simplified approaches for the safety assessment in agreement with Italian Code for the Built Heritage recommendations [28], non-linear static (pushover) and full non-linear dynamic analyses. In all cases, full 3D detailed FE models of both towers have been used. When dealing with the non-linear static and dynamic analyses, a sophisticated damage plasticity model with distinct damage parameters in tension and compression has been adopted.

From the numerical results, both the role played by the actual geometry and the insufficient resistance of the masonry material are envisaged, also in light of the actual failure mechanisms experienced in the real seismic event. In all cases, the numerical analyses provide a valuable picture of all possible failure mechanisms, thus giving useful hints for reconstruction. In particular, the agreement between the actual collapse modes and the crack patterns provided by the non-linear dynamic analyses is worth noting.

Comparing the assumed rehabilitation methodologies, it comes out that little damage develops when lime mortar is used, whereas less promising results are obtained when injections with cement mortar are used. This looks, therefore, to be in line with one of the modern restoration principles, which is considered as a priority by the scientific community, i.e., the beneficial role played by the conservation of the material characterizing the original structural assets. One of the main outcomes of this research may therefore be in the awareness that interventions based on less strong materials provide a considerable reduction of the seismic vulnerability, respecting at the same time the original structural functions of the different items. All should be carefully considered in view of the future reconstruction of both monuments. Not less important is the concept that, in relation to the preservation of such kind of monuments all over the national territory, standard maintenance

programs of the mechanical properties of the structural materials could be sufficient.

References

[1] M. Calzolari, M. Righini, G. Tusini, Le rocche di Finale in età Estense, Gruppo studi bassa modenese, Modena (Italy), 2009.
[2] NTC, Nuove norme tecniche per le costruzioni, Ministero delle Infrastrutture (GU n.29 04/02/2008), Rome, Italy, 2008 (14.01.08).
[3] Circolare 617, Circolare del 2 febbraio 2009 Istruzioni per l'Applicazione delle Nuove Norme Tecniche sulle Costruzioni di cui al Decreto Ministeriale 14 gennaio 2008, 2009.
[4] OPCM 3274, Ordinanza del Presidente del Consiglio dei Ministri n.3274 20/03/2003: Elementi in materia di criteri generali per la classificazione sismica del territorio nazionale e di normative tecniche per le costruzioni in zona sismica e successivi aggiornamenti, 2003.
[5] OPCM 3431, Ordinanza del Presidente del Consiglio dei Ministri n.3431 09/05/2005, Ulteriori modifiche ed integrazioni all'OPCM 3274/03, 2005.
[6] L. Petti, A. Lodato, Preliminary Spatial Analysis and Comparison between Response Spectra Evaluated for Emilia Romagna Earthquakes and Elastic Demand Spectra According to the New Seismic Italian Code, Salerno University Internal Report, Salerno (Italy), 2012.
[7] M. Acito, M. Bocciarelli, C. Chesi, G. Milani, Collapse of the clock tower in Finale Emilia after the May 2012 Emilia-Romagna earthquake sequence: numerical insight, Eng. Struct. 72 (2013) 70–91.
[8] A.H.P. Maurenbrecher, K. Trischuk, M.Z. Rousseau, M.I. Subercaseaux, Repointing mortars for older masonry buildings-site considerations, Constr. Technol. Update 67 (2008) 1–6.
[9] M.R. Valluzzi, F. Da Porto, C. Modena, Behavior of multi-leaf stone masonry walls strengthened by different intervention techniques, in: Proc. SAHC 2001, Structural Analysis of Historical Constructions, Guimaraes (Portugal), 2001, pp. 1023–1032.
[10] D. Hadzijanev, Mohr-Coulomb Parameters for Modelling of Concrete Structures, Plaxis Bullettin, Issue 25, Article 2, 2009, pp. 12–15, Spring 2009.
[11] STRAUS7®, Theoretical Manual-Theoretical Background to the Strand7 Finite Element Analysis System, 2004.
[12] ABAQUS®, Theory Manual, Version 6.6, 2006.
[13] E Monti di Sopra, Modelli a Danno e Plasticità per l'analisi di elementi strutturali in muratura (PhD thesis), Trieste University, Trieste (Italy), 2009.
[14] P.B. Lourenço, Experimental and Numerical Issues in the Modelling of the Mechanical Behavior of Masonry, Structural analysis of Historical Constructions, CIMNE, 1998, pp. 57–91.
[15] L. Binda, C. Tiraboschi, G. Mirabella Roberti, G. Baronio, G. Cardani, Experimental and Numerical Investigation on a Brick Masonry Building Prototype. Part I, Technical University of Milan Internal Report, Milano (Italy), 1995.
[16] L. Binda, C. Tiraboschi, G. Mirabella Roberti, G. Baronio, G. Cardani, Experimental and Numerical Investigation on a Brick Masonry Building Prototype. Part II, Technical University of Milan Internal Report, Milano (Italy), 1995.
[17] H.B. Kaushik, D.C. Rai, S.K. Jain, Uniaxial compressive stress-strain model for clay brick masonry, Curr. Sci. 92 (4) (2007) 497–501.
[18] H.B. Kaushik, D.C. Rai, S.K. Jain, Stress strain characteristics of clay brick masonry under uniaxial compression, J. Mater. Civ. Eng. 19 (2007) 728–739.
[19] A. Borri, Manuale delle murature storiche, vol. 2, DEI, Roma, Italy, 2011.
[20] A.W. Hendry, Structural Masonry, first ed., Macmillan Education Limited, London (UK), 1990.
[21] A. Borri, G. Cangi, A. De Maria, Caratterizzazione meccanica delle murature (anche alla luce del recente sisma in Emilia) e interpretazione delle prove sperimentali a taglio, in: Proc. ANIDIS Congress, Associazione Nazionale Italiana Di Ingegneria Sismica, Padua, 30 June–4 July 2013, Padua (Italy), 2013.
[22] M. Corradi, A. Borri, A. Vignoli, Experimental study on the determination of strength of masonry walls, Constr. Build. Mater. 17 (2003) 325–337.
[23] G. Milani, S. Casolo, A. Naliato, A. Tralli, Seismic Assessment of a medieval masonry tower in Northern Italy by limit, nonlinear static, and full dynamic analyses, Int. J. Archit. Heritage Conserv. Anal. Restor. 6 (5) (2011) 489–524.
[24] G. Milani, Lesson learned after the Emilia Romagna, Italy, 20–29 May 2012 earthquakes: a limit analysis insight on three masonry churches, Eng. Fail. Anal. 34 (2013) 761–778.
[25] M. Corradi, C. Tedeschi, L. Binda, A. Borri, Experimental evaluation of shear and compression strength of masonry wall before and after reinfocement, Constr. Build. Mater. 22 (2007) 463–472.
[26] Rhino, Stand-alone, NURBS-Based 3-D Modeling Software, 2007. <http://www.rhino3d.com/>.
[27] M, Capister, A Manini, Analisi del collasso e dei requisiti di vulnerabilità sismica della Torre dei Modenesi e del Mastio del Castello di Finale Emilia (MSc thesis), Technical University of Milan, Milano (Italy), 2013.
[28] Linee guida per la valutazione e la riduzione del rischio sismico del patrimonio culturale, Ministero per i beni e le attività culturali MiBAC, Italy, 2011.
[29] P. Fajfar, A nonlinear analysis method for performance-based seismic design, Earthquake Spectra 16 (3) (2000) 573–592.
[30] T. Albanesi, C. Nuti, Analisi statica non lineare (Pushover), University La Sapienza in Rome Internal Report, Roma (Italy), 2007.